UNIVERSIDADE FEDERAL DO RIO GRANDE DO SUL
INSTITUTO DE INFORMÁTICA
PROGRAMA DE PÓS-GRADUAÇÃO EM COMPUTAÇÃO

LIZETH ANDREA CASTELLANOS BELTRAN

Volumetric Visualization of Confocal Datasets Obtained from Bile Duct Samples

Thesis presented in partial fulfillment
of the requirements for the degree of
Master of Computer Science

Advisor: Carla Maria Dal Sasso Freitas
Coadvisor: Altamiro Amadeu Susin

Porto Alegre
March 2015

CIP – CATALOGING-IN-PUBLICATION

Castellanos Beltran, Lizeth Andrea

Volumetric Visualization of Confocal Datasets Obtained from Bile Duct Samples / Lizeth Andrea Castellanos Beltran. – Porto Alegre: PPGC da UFRGS, 2015.

60 f.: il.

Thesis (Master) – Universidade Federal do Rio Grande do Sul. Programa de Pós-Graduação em Computação, Porto Alegre, BR–RS, 2015. Advisor: Carla Maria Dal Sasso Freitas; Coadvisor: Altamiro Amadeu Susin.

1. Bile duct. 2. Confocal images. 3. Image processing. 4. Direct volume rendering. 5. Transfer functions. I. Dal Sasso Freitas, Carla Maria. II. Amadeu Susin, Altamiro . III. Título.

"To be conscious that we are ignorant
is a great step to knowledge."
— Benjamin Disraeli, 1845

ACKNOWLEDGMENTS

Firstly, a special thank to my family for your infinite love and patience, even living so away.

I would like to thank my advisor, Carla Freitas for his endless help for support this research. She also has spent many hours helping me with all the difficulties that I had as a foreign student. Special thanks also to my co-advisor Altamiro Susin, for his suggestions, his friendship and for welcoming me in his lab. I am also grateful to the hepatologists and researchers: Jorge Bezerra, Pranavkumar Shivakumar, Jorge Luiz dos Santos and Carolina Uribe, they have given me all the medical support for this research.

Thanks to the Federal University of Rio Grande do Sul (UFRGS), the Institute of Informatics (INF) for the high academic quality and thanks also to the CAPES for the partial financial support. I also acknowledge to my fellows in the Visualization, Interaction and Computer Graphics Lab to provide a great company, for help me with suggestions for my research and my Portuguese. Thanks to the teachers: Claudio Jung, Jorge Ortiz and Said Pertuz for their suggestions and help. I am so grateful with Cristiano and Priscila for your friendship while I was away from home. Finally, I would like to express my immense gratitude to Emmanuell Díaz for his encouragement and his advices along the last years.

ABSTRACT

The visual exploration of bile ducts in the liver is of relevant clinical interest, as it provides information related to the Biliary Atresia, a disease of unknown origin, which eventually leads to a liver transplant or ultimately to death. The only physical known evidence of biliary atresia is the obstruction of the bile ducts. However, the study of this disease has been limited by the inability to observe the bile duct in patients at early stages of the disease. Moreover, very little is known about the internal structure of the bile duct. In recent years, confocal microscopy, a technique that allows to obtain 3D image datasets from biological samples, has been used in medical experiments for studying the anatomical internal structure of bile ducts.

We are interested in supporting the study of these structures through volumetric visualization of bile ducts images. In this work, we propose a data flow pipeline capable of processing and rendering datasets of confocal images using The Visualization ToolKit - VTK. The pipeline was built as two consecutive stages. We propose a first stage for denoising and enhancing the relevant structures of sample based on filtering in the frequency domain and anisotropic diffusion. We use the dataset preprocessed in this way for applying a direct volume rendering technique in a second stage based on transfer functions to visualize the bile duct structures. Our results have shown that volumetric visualization together with an adequate pre-processing of the confocal images allow experts to visualize the regions of interest in the bile ducts, improving details that are hardly visualized in the original data.

Keywords: Bile duct. confocal images. image processing. direct volume rendering. transfer functions.

Visualização Volumétrica de Imagens Confocais de Dutos Biliares

RESUMO

A exploração visual dos dutos biliares é de relevante interesse clínico, pois fornece informação relacionada com a Atresia Biliar (AB). A AB é uma doença cujas causas ainda permanecem desconhecidas e que eventualmente leva a um transplante de fígado ou, nos casos mais avançados da doença, leva a óbito do paciente. A única evidência física conhecida até agora da existencia de AB é a obstrução das vias biliares. No entanto, o estudo desta doença tem sido limitado pela incapacidade de analisar o duto biliar de pacientes em estágios precoces da doença e muito pouco se sabe sobre a estrutura interna do duto biliar. Nos últimos anos, a microscopia confocal, uma técnica que permite a obtenção de conjuntos de dados 3D de amostras biológicas, tem sido utilizada em experiências médicas para estudar a estrutura interna e anatômica dos dutos biliares. Neste trabalho, é objetivo apoiar o estudo dessas estruturas através da visualização volumétrica de imagens dos dutos biliares. É proposto um pipeline de fluxo de dados capaz de processar e "renderizar"conjuntos de dados de imagens confocais utilizando o VTK (do inglês The Visualization ToolKit). O pipeline foi construído em duas etapas principais e consecutivas. Uma primeira etapa tem o objetivo de remoção de ruído e realce das estruturas relevantes por meio de filtragem no domínio da freqüência e difusão anisotrópica. O conjunto de dados assim pré-processado é usado com técnicas diretas de visualização de volumes baseadas em funções de transferência para exibir as estruturas dos dutos biliares. Os resultados mostram que a visualização volumétrica em conjunto com um pré-processamento adequado das imagens confocais permite evidenciar as regiões de interesse nos dutos biliares e melhora detalhes que são dificilmente visualizados nos dados originais.

Palavras-chave: Duto biliar, imagens confocais, procesamento de imagens, visualização volumétrica, funções de transferência.

LIST OF ABBREVIATIONS AND ACRONYMS

2D	Two-dimensional
3D	Three-dimensional
BA	Biliary Atresia
CT	Computed Tomography
DVR	Direct Volume Rendering
MRI	Magnetic Resonance Imaging
VTK	Visualization Toolkit
PBGs	Peribiliary Glands
PVP	Peribiliary Vascular Plexus

LIST OF FIGURES

LIST OF TABLES

CONTENTS

1 INTRODUCTION

Along the years, medical images have been used for the analysis and study of biological structures. However, it is well known that it is difficult to analyze the three-dimensional structure of inner structures by viewing individual 2D slices (DREBIN; CARPENTER; HANRAHAN, 1988). To overcome this limitation, since the early 90's, volumetric visualization techniques have been developed to create a single three-dimensional representation of such structures for supporting biological and medical analysis.

Some examples of techniques employed to obtain the medical datasets used in volumetric visualizations include Computed Tomography (CT), Magnetic Resonance (MR) and Confocal Microscopy. CT and MR have been typical techniques used mainly to capture data for the analysis of structures such as organs and bones. These two image acquisition techniques are focused on the reconstruction of macro structures, however they do not have the adequate resolution to capture details of micro structures. On the other hand, confocal microscopy has become an invaluable tool for a wide range of research on structures such as cells because it has the adequate optical properties to collect microscopic samples.

Confocal microscopy offers several advantages over conventional optical microscopy, including the ability to control the depth of field and the capability to collect serial optical slices from biological specimens (CLAXTON; FELLERS; DAVIDSON, 2006a). Because of those advantages confocal microscopy has been used in research to obtain 3D datasets, mostly from cells (CLAXTON; FELLERS; DAVIDSON, 2006b). However, it is still a relatively young field. The modern era of this technique started in 1985 and, since then, its usage by biologists has increased year by year (PRICE; JEROME, 2011).

A recent application of confocal microscopy is the analysis of bile duct samples for studying the causes of a disease of unknown origin called biliary atresia (BA) (DIPAOLA et al., 2013). This disease affects the bile ducts and has been studied by medical experts, in this case by hepatologists (SANTOS; CARVALHO; BEZERRA, 2010). Although in the last years some traditional non-invasive techniques

such as CT, MR and ultrasound have been used to acquire images of bile ducts for their analysis, these techniques do not offer details about the bile duct tissue and their internal structures. Moreover, the study of BA has been limited by the inability to analyze biliary tissues from patients at early phases of disease. As a consequence of this lack of information about bile ducts, a medical research team from the Cincinnati Children's Hospital has proposed some experiments in mice to study the anatomy of the bile ducts (DIPAOLA et al., 2013). They have studied the staining process used in confocal microscopy and have adapted those techniques to be applied to macro structures such as the bile ducts. Confocal microscopy is traditionally used on micro structures such as cells. The challenge of the proposed research on the Cincinnati Children's Hospital was made the animal model of atresia using macro structures such as the mouse bile ducts.

1.1 Motivation and Objective

Our work is motivated by the need of the research group on biliary atresia at the Hospital de Clinicas de Porto Alegre (HCPA), which started to study the technique under development at the Cincinnati Children's Hospital. The experts at the HCPA would like to employ volumetric visualization and shape analysis to verify hypotheses about the causes of biliary atresia, by inspecting samples taken from mice along the development of the disease.

Actually, both groups are scientific partners, and we benefited from this by the possibility of obtaining experimental datasets. However, despite the American group succeeded in obtaining samples using confocal microscopy, their approach imposes some challenges associated to the bile duct staining as well as the image datasets acquisition. Despite the effort dedicated to the samples preparation and the image acquisition itself, it still is necessary an adequate computational support for the processing and visualization of the acquired confocal datasets.

The purpose of this work is to help the hepatologists in a better understanding of the internal and external bile duct structures using confocal images. In order to successfully achieve this goal, we propose the use of image processing techniques to enhance the confocal images, and volumetric visualization techniques to create a projection of the bile duct dataset in a 3D space so the experts can examine the shape and distribution of the structures composing the bile ducts.

Our main contribution is a data flow pipeline capable of processing confocal data and producing a volumetric visualization of the bile ducts improving details that are hardly visualized in the original data.

1.2 Structure of the Dissertation

The remaining text of this dissertation is arranged as follows. Chapter 2 introduces basic concepts on confocal microscopy and briefly discusses related works. Chapter 3 presents a detailed description of the motivating problem. Chapter 4 presents the proposed pipeline for the visualization of confocal data from bile ducts and presents the algorithms and techniques used in our implementation. Results are reported and discussed in Chapter 5, and finally, in Chapter 6, we draw our conclusions and explain future work.

2 BACKGROUND AND RELATED WORK ON CONFOCAL DATA

This work is focused on the processing and visualization of bile duct confocal images. Because of this focus, it is important to understand some operating principles of confocal microscopes. This knowledge allows us an adequate comprehension about the advantages and limitations associated to the acquisition device, which affects directly the data we are processing. Confocal microscopy data have their own characteristics, which differ from other biomedical data such as CT or MR (WAN et al., 2012).

The characteristics of a confocal microscope also offer several advantages over conventional optical microscopy. In this chapter we introduce some basic principles to understand this recent technique and the reasons for using it in this work.

Moreover, due to the 3D nature of confocal datasets, the straightforward way to render them is using volumetric visualization techniques. In this chapter we also review the related work about visualization of confocal datasets.

2.1 Fundamental Concepts about Confocal Microscopes

To effectively use a confocal microscope, researchers must have an understanding of some important topics, including fluorescence theory, sample preparation, and fluorescent antibody interactions.

Fluorescence is the property of some atoms and molecules to absorb light at a particular wavelength and to subsequently emit light of longer wavelength after a brief interval (Michael W. Davidson., 2014). This property provides a specific, high contrast signal that maximally exploits the ability of the confocal microscope to remove out-of-focus light (PRICE; JEROME, 2011). In a confocal microscope (Figure 2.1), images are acquired point-by-point and from selected depths. To gather this information, the light emitted by the laser passes through a pinhole aperture that is situated in a conjugate plane (hence the name confocal) with a scanning point on a sample and a second pinhole aperture positioned in front of the detector. As the

Figure 2.1: Laser Scanning Confocal Microscope.

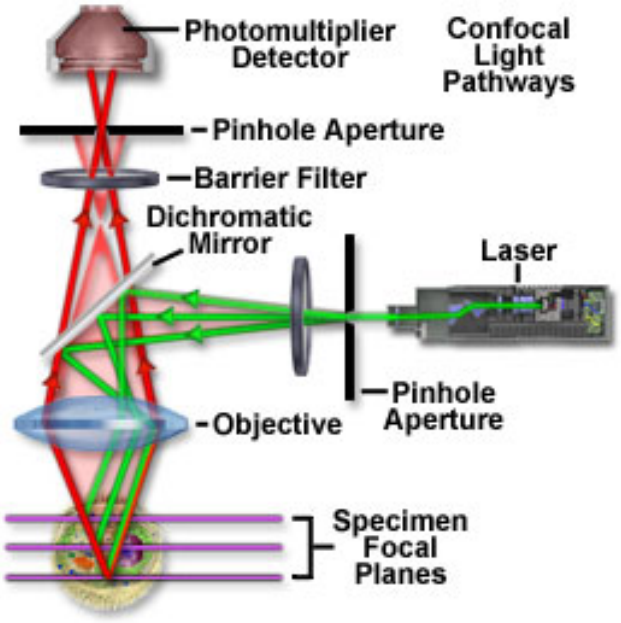

Source: http://www.olympusconfocal.com/theory/index.html

laser is reflected by a dichromatic mirror and scans across a sample in a defined focal plane, secondary fluorescence emitted from points on the sample (in the same focal plane) pass back through the dichromatic mirror and are focused as a confocal point at the detector pinhole aperture(CLAXTON; FELLERS; DAVIDSON, 2006b).

The specimen can be labeled with several appropriate fluorescent antibodies, which allow to mark different tissues or cells. As shown in Figure 2.2, blue, green and red laser lines are used to excite a sample labeled with three fluorescent antibodies. The laser passes through a filter that allows control of the laser intensity. The dichromatic filter separates the higher energy short-wavelength excitation photons from the lower energy long-wavelength photons emitted from the specimen. The laser passes through the scan head and objective lens, and interacts with the sample. The photons emitted from the sample take the reverse path of the excitation photons and pass through the objective and then through the filters. Finally, the photomultiplier tube (PMT) is a detector that collects and records photons of all wavelengths. This complex process allows to obtain high a resolution image of one focal plane, also called slice of the specimen. This process is repeated along the complete depth of the specimen, producing an ordered group of confocal images called stack.

In order to store the acquired data many of the confocal microscopes uses proprietary formats. These machine specific formats allows to acquire and store additional information about the image such as resolution, number of channels and other in-

Figure 2.2: General diagram of the mechanism for collecting signals from a sample labeled with three fluorescent antibodies using three laser beams.

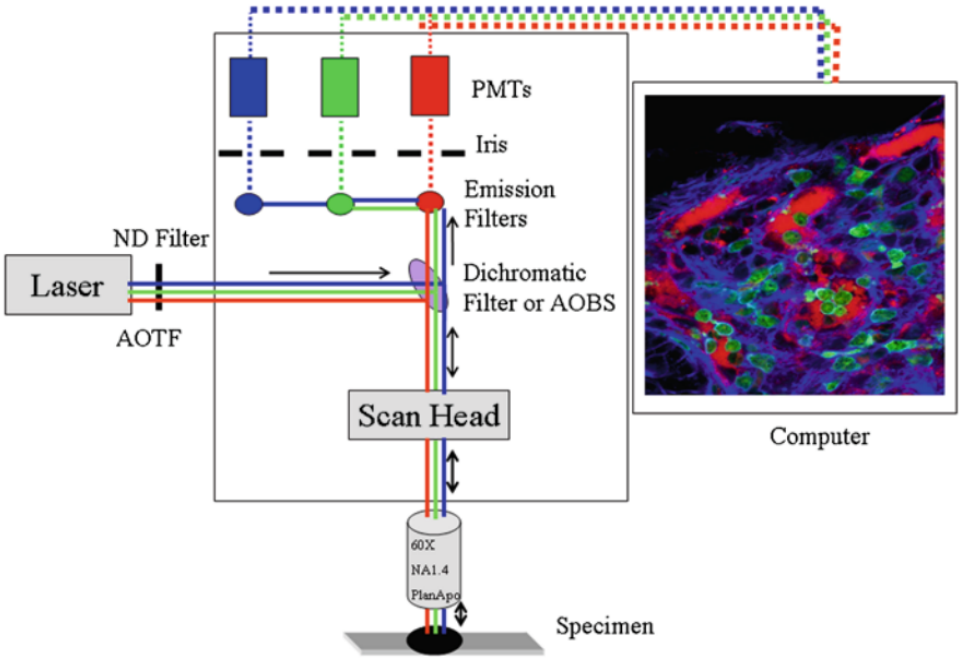

Source: (PRICE; JEROME, 2011)

formation about microscope such as objective and plane spacing. In the case of confocal microscopes, this often includes a wealth of information about the microscope settings used to collect the image. Having information used during image collection is extremely useful. However, the downside of proprietary formats is that they need proprietary software to decode the stored image. This fact makes it difficult to share the images with other researchers (PRICE; JEROME, 2011) or loss of information when converting to another more common format. The Zeiss LSM file format (Laser Scanning Microscope) is an example of such a proprietary format, it is the format of the devices we used to acquire confocal data, we will describe it later in Chapter 4.

Confocal microscopy can be used on fixed samples or on live imaging. Live imaging allows the analysis of dynamic events in real time and avoids some of the artifacts that can be introduced by specimen preservation, but this often comes at a price. Since the specimen is not preserved, the microscopist must ensure that the act of viewing the sample does not introduce artifacts. In many ways, working with fixed material simplifies microscopy imaging. In particular, because the microscopists do not have to worry about keeping the sample alive and healthy. Moreover, a fixed sample is generally more resistant to excitation beam-induced changes. The choice of available fluorescent antibodies is also much greater when working with fixed

Figure 2.3: Representation of a 3D Confocal Dataset.

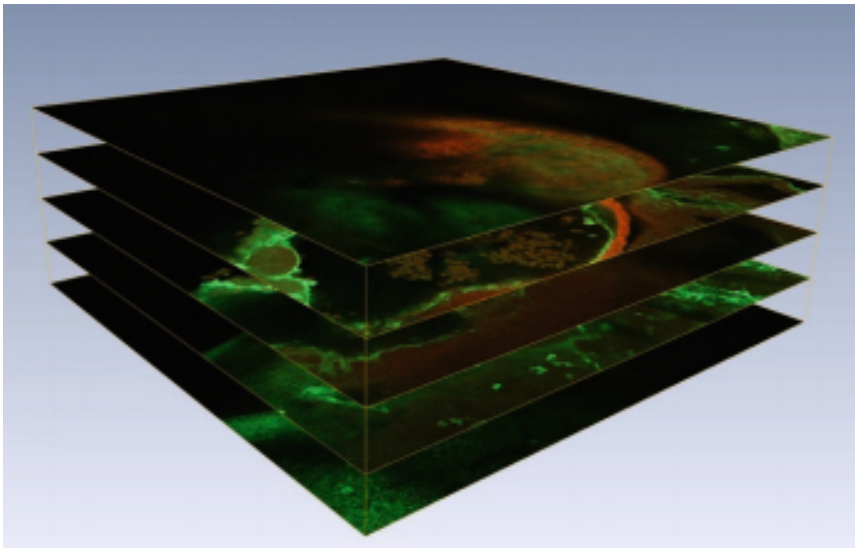

Source: (PRICE; JEROME, 2011)

material. For this reason, the majority of confocal experiments use fixed samples (PRICE; JEROME, 2011).

2.2 3D Confocal Data

By analogy with 2D images, where screen is split up into pixels and the density value of each is represented by a finite number of bits, in a 3D image the unit of information is called a voxel (TORIWAKI; YOSHIDA, 2009). Confocal images are an example of 3D images: confocal data are datasets with aligned images such as shown in Figure 2.3, where each pixel in each slice can be considered a voxel. A voxel represents the smallest unit of volume information.

Visualization strategies are very different in medical images. No single approach fits all the needs, and the different approaches are highly associated with the input image characteristics.

Confocal microscopy data have their own characteristics, which differ from other biomedical data, and directly affects visualization:

- Multichanel data: labeling with different fluorescent proteins and fluorescent dyes yields multi-channel data, with each channel representing a different cell or tissue type. Usually the data in different channels are spatially interwoven, with data from one channel having the highest interest.

- Subtle boundaries: Biologically meaningful boundaries may be only subtly

presented in the confocal data, and may be present in only one channel of the multi-channel data.

- Finely detailed structures: Biomedical techniques such as antibody staining and gene transfer allow delivery of fluorescent dyes to specific cell or tissue types, which can result in very finely detailed structures.

- Visual occluders and noise: Structures irrelevant to the analysis may also be labeled through the fluorescent staining process, resulting in visual occluders that obscure the structures to be visualized. Fine detailed structures can also be obscured by noisy data, due to statistical noise or electronic noise from the scanning device.

- Diversity of density values: The physical meaning of density values is not limited to image subjects and their recordings, but will vary greatly according to the space they are contained in and the measurement (imaging) technologies used, even when the same subject is being treated. An example is given in Table 2.1. According to these factors, the characteristics and content of detected edges, outlines, high density areas, etc., will be very different (TORIWAKI; YOSHIDA, 2009).

Some of these characteristics were relevant for the selection of confocal microscope as an adequate method for image acquisition of the bile ducts used in this work. For example, the use of fluorescent antibodies and the advantage to construct multichannel data, permits a prior segmentation process of the images, in which green channel contain information about some specific structures and red channel

Table 2.1: Examples of meanings of density values in 3D images.

3D Input Image	Meaning of density
X Ray CT Images	Attenuation coefficient of X ray at small volume of an object.
Magnetic Resonance Images	Strength of resonance signals at a small volume element of an object.
Ultrasound Images	Absorption, reflection, or transmission coefficient of ultrasound wave at a small volume element.
Confocal Laser Microscopic Images	Strength of reflected light or distance to the surface of an object.

Source: (TORIWAKI; YOSHIDA, 2009).

contain information about other type of structures. Green and red channel were encoded in the same dataset for postprocessing steps. The fluorescent antibodies also offers more details of the structures presents in the bile duct, which are not possible to see when other medical devices are used for image acquisition.
Confocal microscope also differs of other medical devices by the method to capture density values in a specimen. Table 2.1, contains different meanings of density for each biomedical imaging method and Figure 2.4 illustrates this fact with more details.

Traditional imaging methods such as MR, ultrasound and CT are focused on obtaining a visual representation of macro structures such as bones and organs. For the bile ducts those methods provide a general idea about the shape and size. However, details about the internal bile duct structures are not visible. On the other hand, confocal microscopy is focused on obtaining images of micro structures such as cells and molecules.

One of the challenges of the image acquisition of the bile ducts for this work is that the bile ducts are formed by macro and micro structures. Both, macro and micro structure types are relevant for medical research on the biliary atresia and should be acquired and digitized using an appropriate approach. Confocal microscopy combined with an adequate sample preparation allow the hepatologists to acquire datasets from the bile ducts with better resolution as can be seen in Figure 2.4

2.3 Advantages and Critical Aspects of Confocal Microscopy

Confocal microscopy offers several advantages over conventional optical microscopy (CLAXTON; FELLERS; DAVIDSON, 2006b). The main advantage is depth (Z axis) selectivity. This characteristic permits to acquire the confocal images along three axis on the specimen: x axis (width), y axis (long) and z axis (depth). Advantages of confocal microscope over optical microscopy include:

- Ability to control the depth of field.
- Elimination or reduction of background information away from the focal plane.
- Capability of collecting serial optical slices from the specimen.
- Use of spatial filtering techniques to eliminate out-of-focus light.

There are some factors related to acquisition devices that may affect the quality and quantification of confocal images as shown in Table 2.2.

Some of the factors affecting image quality are directly related with the configuration of the microscope, and can be overcome with an adequate knowledge of

confocal microscopy principles. Other ones are related to the sample preparation. An optimal biological sample preparation for confocal microscopy is very dependent on the cell or tissue type, the labeling technique, and type of data to be collected (PRICE; JEROME, 2011). The staining process and laser light transmission in biological samples are limited when applied to thick sections, resulting in distorted images. So, those factors can affect the images of bile ducts because they are a macro structure. We are unable to overcome this problem because it is part of the bile duct sample preparation, still in an experimental stage by the hepatologists.

Figure 2.4: Comparative between bile duct images obtained from traditional imaging methods and confocal microscopy.

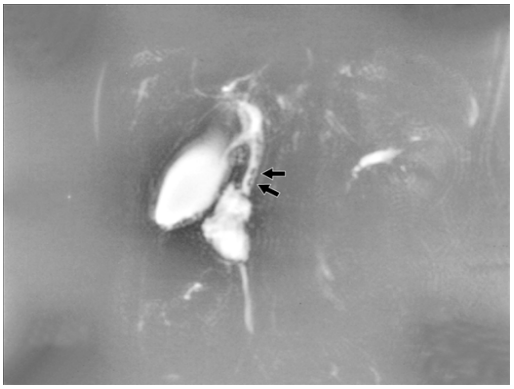

(a) Bile duct obtained from magnetic resonance

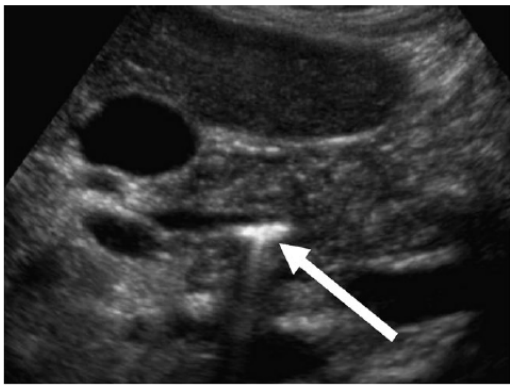

(b) Bile duct in an ultrasound image

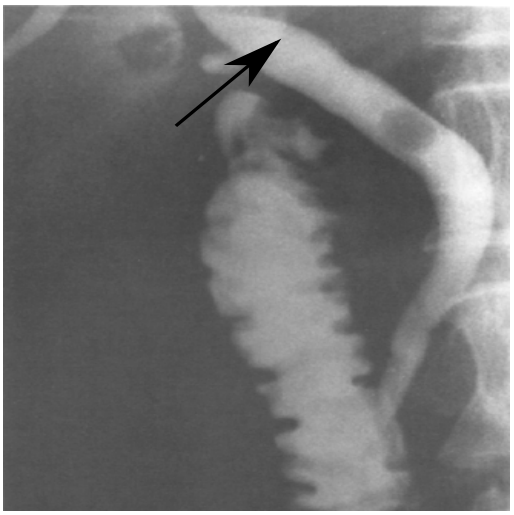

(c) Bile duct in a computed tomography image

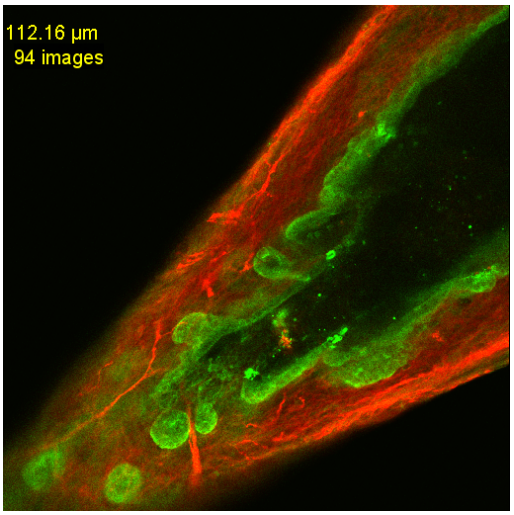

(d) Bile duct in a confocal microscopy image

Source: Figure 2.4a from (DEMARTINES et al., 2000); Figure 2.4b from (HORROW, 2010); Figure 2.4c from (SUZUKI et al., 1983); Figure 2.4d from the author.

Table 2.2: Some factors that may affect the quality and quantification of confocal images.

Microscope, specimen, or image component	Consideration that may affect quantification
Laser unit	Alignment. Instability with age. Efficiency of optical coupling.
Scanning system	Zoom magnification. Raster (pixel) size. Distortions. Environment (stray fields, vibrations).
Microscope objective	Numerical aperture. Magnification. Dipping/immersion lens. Spherical/chromatic aberrations. Cleanliness.
Other optical components	Mirrors. Excitation and emission filters. Coverslips. Immersion oil.
Fluorescent antibodies	Concentration. Quantum efficiency. Saturation state. Loading. Quenching. Reaction rates. Dye/dye interactions.
Pinhole	Alignment. Diameter. Sensitivity. Inherent noise.
Digitization	Linearity - statistical noise.

Source: (TORIWAKI; YOSHIDA, 2009).

There are another challenges that also affect the image quality and that we try to overcome. These are associated to visual occlusion and noise, that may be caused by the fluorescent antibodies and may affect the quality and the information contained in the images. For example, the fluorescent antibodies can also label irrelevant structures in the staining process. The use of two channels of data in the same dataset can also produce visual occlusion and noise. To overcome these factors, we divided the original confocal dataset into two datasets, one containing the red data channel and the other containing the green data channel. We also tested several

techniques to reduce the noise in the original datasets, and selected those that do not affected the relevant structures. These techniques will be explained in Chapter 4.

2.4 Visualization of Confocal Datasets

Works with multidimensional confocal datasets composed by images taken from microscopes include biology studies such as dynamics of microtubule spindles during mitosis (INOUÉ, 2008), profiling gene expression of cells (RUBEL et al., 2010; RAFALSKA-METCALF; JANICKI, 2007; LONG et al., 2009), screening phenotypic data and reconstructing the morphology of neurons (PENG et al., 2010; PENG; LONG; MYERS, 2011; MEIJERING et al., 2004). However, most of those studies are performed with 2D images, probably due to its simplicity for biologists (LONG; ZHOU; PENG, 2012).

Contrasting with those works, our research is focused on 3D images and we need to take in consideration all the images contained in the dataset. Volume rendering of microscopic data is an ongoing research topic due its inherent visual complexity (BEYER et al., 2013). In addition to this complexity, confocal microscopy produces multi-channel data, and this creates a large amount of information.

Transfer functions are the key to volume rendering of medical datasets. Since visualization strategies are very different, some approaches can use one-dimensional transfer functions and, in contrast, other approaches can use multidimensional transfer functions. One-dimensional (1D) transfer functions, which maps image data values into color and opacity, are the most explored approach. However, such transfer functions take into account only the scalar voxel value and have limited classification power. To improve this limitation, the gradient magnitude is commonly used as second dimension to guide the transfer function in distinguishing internal structures (KINDLMANN; DURKIN, 1998). Gradient magnitude makes it possible to differentiate between homogeneous regions and transition regions allowing us to isolate areas of interest more effectively (KNISS; KINDLMANN; HANSEN, 2001) (JOE; GORDON; CHARLES, 2002). Several works have explored the gradient approach to guide the volume rendering (LUM; MA, 2004), (PINTO; FREITAS, 2008). However, in confocal data this approach has not been studied extensively (KIM, 2011).

Despite the difficulties of working with multi-channel data, to the best of our knowledge, there are only two works that apply gradient-based transfer function for confocal data (WAN et al., 2012) (KIM et al., 2010). Wan et al. proposed an application for enhancement of confocal microscopy visualizations but their approach was aiming at a specific research on neuron cells (WAN et al., 2012). Kim et al. used gradient information combined with other properties such as curvature and

texture to guide the transfer functions in brain cells (KIM et al., 2010).

As can be observed, visualization strategies and approaches of the previous works have been applied to cells. Our work includes a challenge associated to data because we have a macro-structure (the bile duct), and there are some factors associated to the staining process and image acquisition that affect the image quality in thick specimens.

3 PROBLEM DESCRIPTION

The studies searching for the causes of biliary atresia have been limited by the inability to explore the bile duct in the early phases of the disease. Thus, understanding the bile duct anatomy is a relevant task in these studies by hepatologists, especially because the internal anatomy of the bile ducts is still unknown.

Figure 3.1 illustrates an example of a normal and an atypical bile duct. Red arrows shown obstructions in the bile duct. When those obstructions appears, it is the only external physical evidence of the biliary atresia presence known to date. However hepatologists theorizes about what is happening in the internal structure of the bile duct.

Currently, there are no public datasets of bile ducts as we need for developing our work. Moreover, even the datasets we have obtained from experts are not ready for visualization, and it is necessary to employ adequate techniques for pre-processing them. In this chapter we describe the research problem as well as the challenges regarding image processing and volumetric visualization.

3.1 Confocal Datasets of Bile Ducts

In confocal microscopy, there is no single best method of preparing a sample that can accommodate all types of samples, all possible methods of staining specific structures, and all possible modes of imaging. Optimum biological sample preparation for confocal microscopy is very dependent upon the cell or tissue type, the labeling technique, and type of data to be collected (PRICE; JEROME, 2011).

Confocal microscopy has been used for studying microscopic structures. The technique developed at Cincinnati Children's Hospital Center made possible its application in macroscopic structures such as the bile ducts (DIPAOLA et al., 2013). The bile duct is a macro-structure, which is composed by many micro-structures (cells and tissues). In order to acquire and analyze three-dimensional structural information of the bile duct, the 3D structural relationships must be preserved during the sample preparation. Because of the added need to preserve the 3D structure for

Figure 3.1: General representation of a normal and an atypical bile duct.

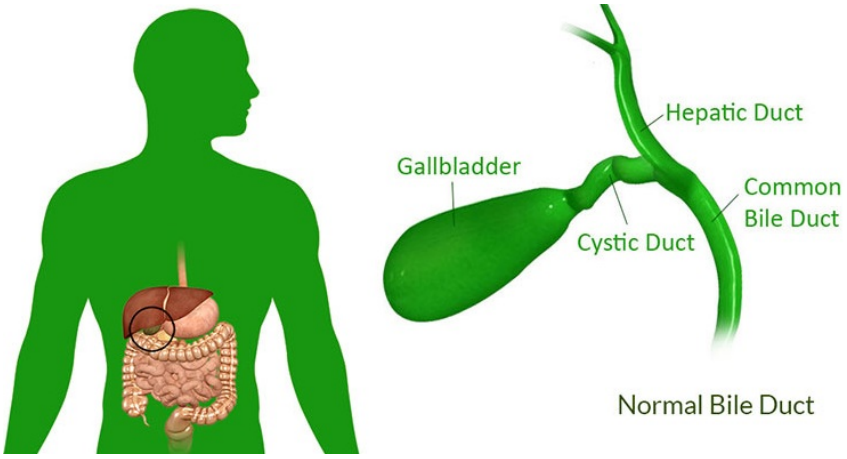

(a) Normal bile duct

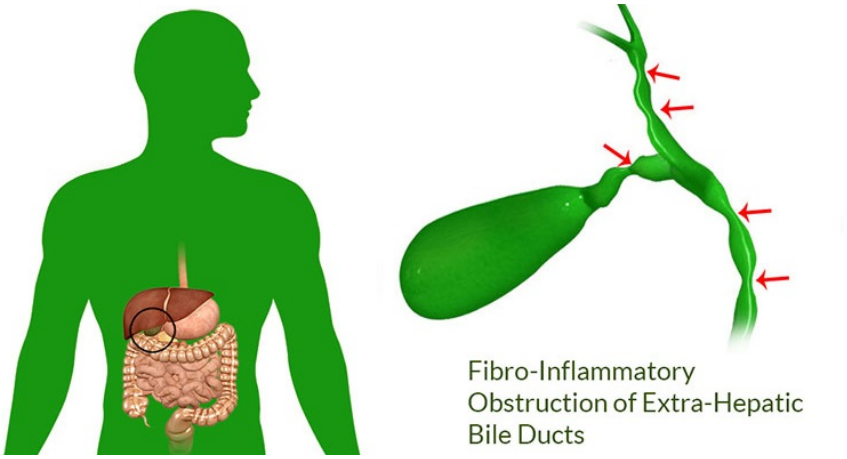

(b) Bile duct with biliar atresy

Source: http://pixgood.com/biliary-atresia.html

confocal images, methods suitable for preparing samples for optical microscopy must often be altered to accommodate the additional demand of preserving relationships in the third dimension. This fact imposes an initial challenge that is the need of treating many variables in the specimen preparation process as well as during staining process. Another challenge is that the Signal-to-Noise-Ratio (SNR) of the slices of the stack obtained using confocal microscopes decreases with increasing depth (RAMESH; OTSUNA; TASDIZEN, 2013). Hence, the quality of the fluorescence decreases with increasing depth. For typical experiments using biological cells this problem is not that relevant, because the cells are thinner than macroscopic struc-

tures. However in experiments that use macro structures, such as the bile duct, this challenge affects the image quality because the bile duct has larger depth area than the microscopic structures.
The input dataset used in this work was obtained from our partners, which are at an initial phase of their experiments with mice bile ducts and confocal microscopy. Those datasets contain images of serial slices in the adequate order to permit us to construct volumetric visualizations of all bile duct. Figure 3.2 shows a mouse bile duct extracted and treated by the hepatologists. This bile duct has been dyed with two fluorescent antibodies, (α-tubulin) and (Cytokeratin CK), after this stage the bile duct is ready for use in the confocal microscope.

Figure 3.3 represents a 2D view of the bile duct. Each slice in the dataset has 512 x 512 pixels, and the stack is composed by a total of 192 slices. So, the dimensions for the dataset are 512 x 512 x 192.

In this visualization (Fig. 3.3), we selected the slice number 94 of a dataset. We selected this 2D view to show the variety of structures and to perform a manual identification of those structures in collaboration with the hepatologists.

The resulting dataset then consists of two channels. The first one (red) represents the blood vessels with (α-tubulin staining) (Figure3.3a) and the second one (green) the peribiliary glands (PBGs) with CK staining (Figure3.3b). We observed in these images that PBGs do not have a well-defined structure. The bile duct can contain isolated glands, but it is also possible to find groups of glands contained within the duct wall as in Figure 3.3c.

Based on experiments, (DIPAOLA et al., 2013) discovered that PBGs elongate to form complex networks that course and branch within the bile duct walls. PBGs are relevant for the hepatologists' studies because they are described in several animal species including mice and humans. Moreover, PBGs' cells express a range of proteins, which may be relevant to healthy bile duct physiology (HOPWOOD; WOOD; MILNE, 1988) (TERADA; KIDA; NAKANUMA, 1993). Also, besides shape, they want to verify if PBGs change in size, number and distribution because of this disease.

In addition to the PBGs, there are another important structures to visualize. The blood vessels in the red channel form the structural layer of the bile duct (Figure 3.3c). Regarding these structures, the hepatologists have proposed some hypotheses, which relate to possible disturbances in the network of vessels with the existence of a biliary atresia.

All their assumptions are expected to be verified in a more advanced stage of their experiments, and our visualization dataflow aims to help them in these analyses at different stages of biliary atresia.

Figure 3.2: A mouse bile duct ready to use in confocal a microscope

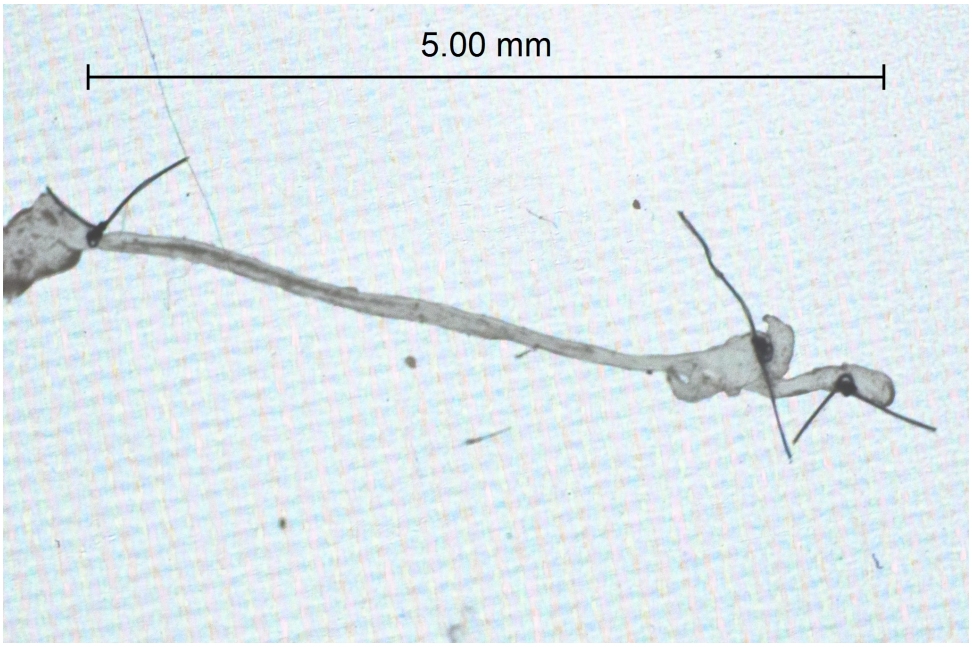

Source: Author

3.2 Shortcomings of Current Software Solutions

Confocal microscopy devices use proprietary software. However, the focus of the device-included software is essentially the image acquisition and not the pre-processing of the data after acquisition. The 2D original slices can be explored by the hepatologists using this software, but there is a lack of more elaborated techniques for processing the datasets to enhance the data and generate volumetric visualizations that would show more details about the structures. For example, Figure 3.4 shows a 2D view of a bile duct with 2 channels of fluorescence. It is difficult to observe the 3D structure of the bile duct by viewing individual slices, and for this reason this work has focused in the volumetric visualization of confocal datasets.

Figure 3.5 and Figure 3.6 present a general volumetric visualization obtained with the software of the microscope. Those visualizations do not allow differentiating the transitions between the structures present in the volume.

Usually, the proprietary software allows simple contrast enhancement of 2D images, and the volumetric visualization is obtained with a simple 1D transfer function, that maps the scalar voxel value to a color. However this proprietary software produces generic volumetric visualizations and not permit a more detailed processing to enhance the quality of the images acquired.

Figure 3.3: 2D view of a Bile Duct Dataset obtained from confocal microscopy: the red channel encodes the blood vessels, while the green one encodes the peribiliary glands. Each encoding is done using two fluorescent antibodies.

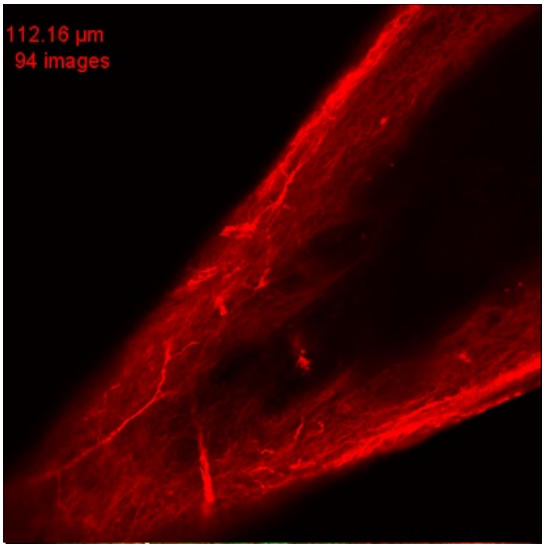

(a) Red channel

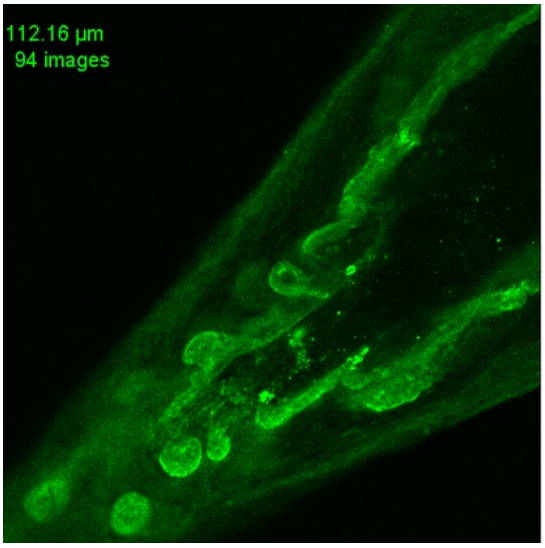

(b) Green channel

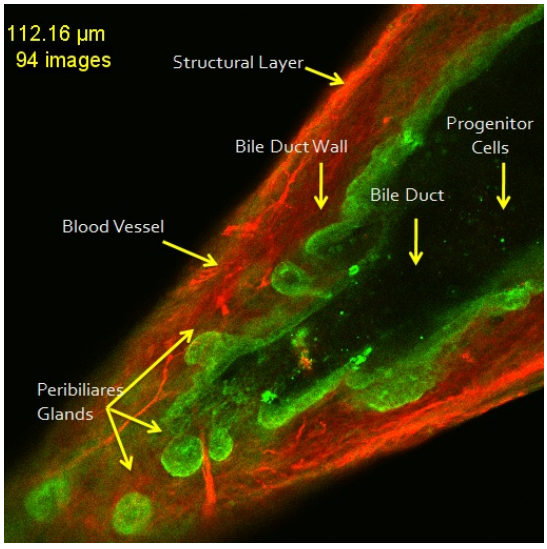

(c) Dataset with green and red channel

Source: Author

Figure 3.4: 2D bile duct view using ZEN 2009 Light Edition Software from Confocal Microscope.

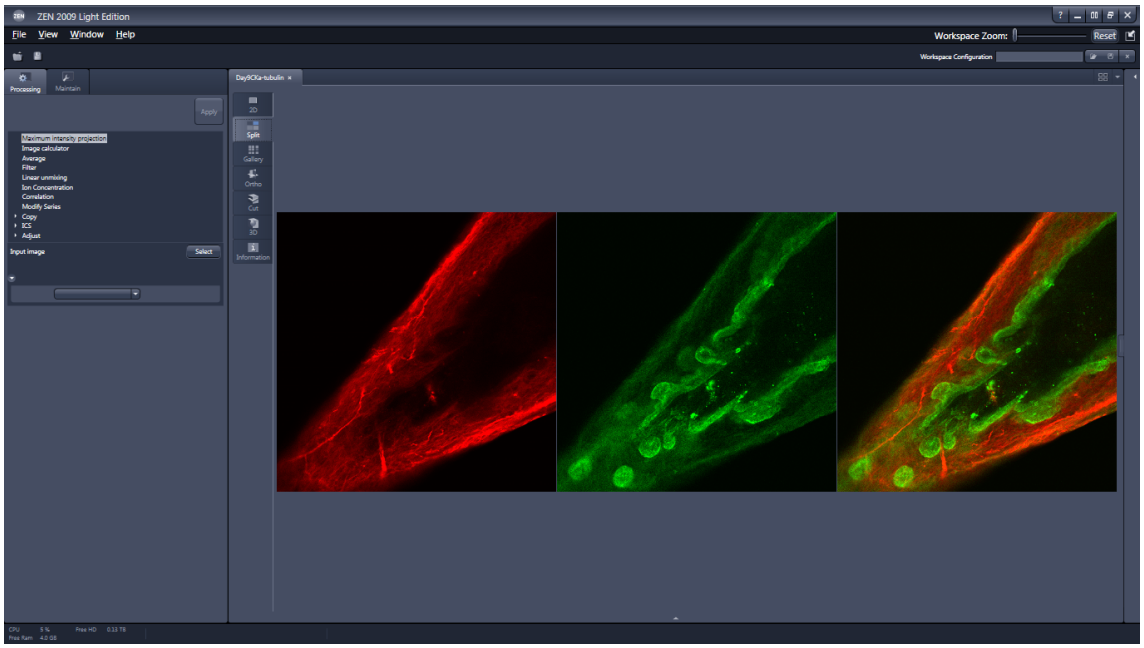

Source: (ZEISS, Jena: Zeiss, 2009)

Figure 3.5: 3D reconstruction of green channel using ZEN 2009 Light Edition Software .

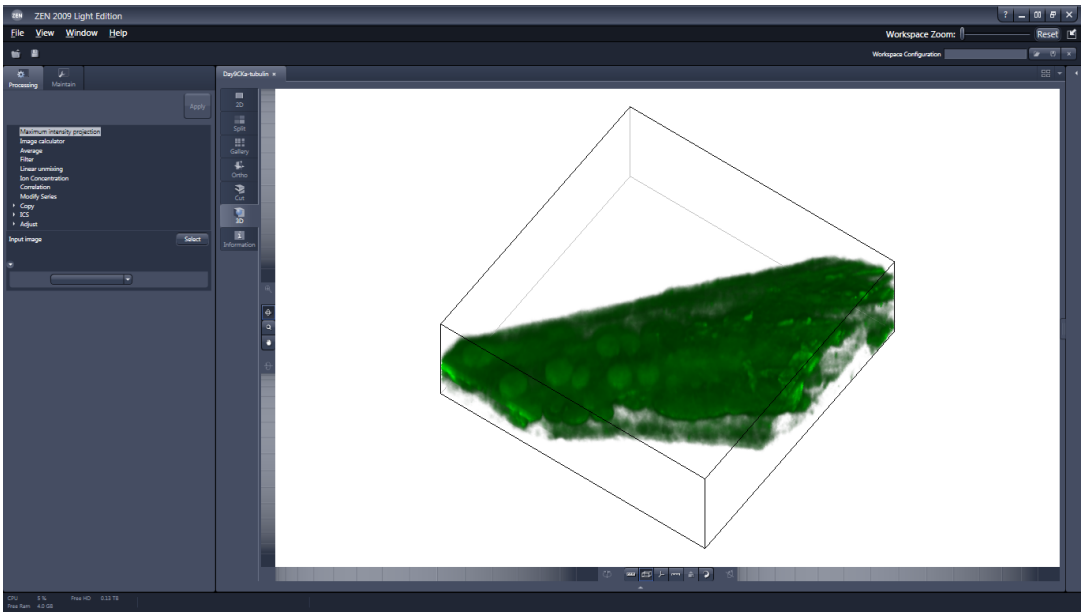

Source: (ZEISS, Jena: Zeiss, 2009)

Figure 3.6: 3D bile duct reconstruction of red channel using ZEN 2009 Light Edition Software..

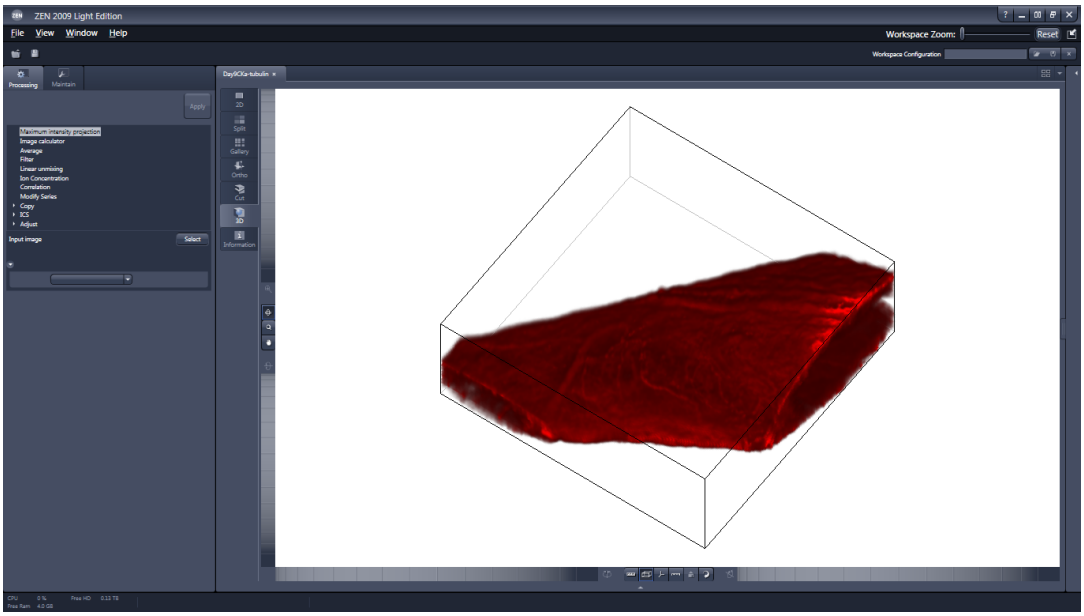

Source:(ZEISS, Jena: Zeiss, 2009)

4 PIPELINE FOR VISUALIZING CONFOCAL DATASETS OF BILE DUCTS

It is difficult for hepatologists to have a direct comprehension of 3D confocal images. The use of appropriate display techniques is therefore extremely important to allow a better understanding of these data. Due to the inherent 3D structure of confocal images, direct volume rendering techniques are the straightforward solution.

However, after several tests, we realized that it is necessary to apply an adequate pre-processing step to the original datasets to obtain meaningful information. Approaches for image pre-processing of medical images are very dependent of the data. To the best of our knowledge, related work on confocal data are not focused on three dimensional image processing. Because of the limited information in our specific area of study (confocal data), we decided to run several tests with different medical image processing techniques and volume rendering techniques.

We then selected the techniques that gave satisfactory visual results according to our medical expert partner, and construct a pipeline to process our data using these techniques in an appropriate order. In this chapter we present the pipeline and the fundamental aspects about the techniques we selected for the implementation of our tool.

4.1 Image processing Techniques

Due to the characteristics of confocal images it is necessary to improve the acquired data by enhancing the image quality.

The green channel is the most noisy channel of our datasets. In this channel the relevant structures of study are the glands (not perfect circular or torus shaped), which are distributed along the inner wall of the duct as shown in Figure 4.1a. However, the glands are not well defined and include noise of the bile wall as shown with more detail in Figure 4.1b. In addition to the noise, the glands and the bile duct wall are very close to each other, and because of this, it is difficult to distinguish these two types of structures.

Figure 4.1: 2D view of noise in original green channel.

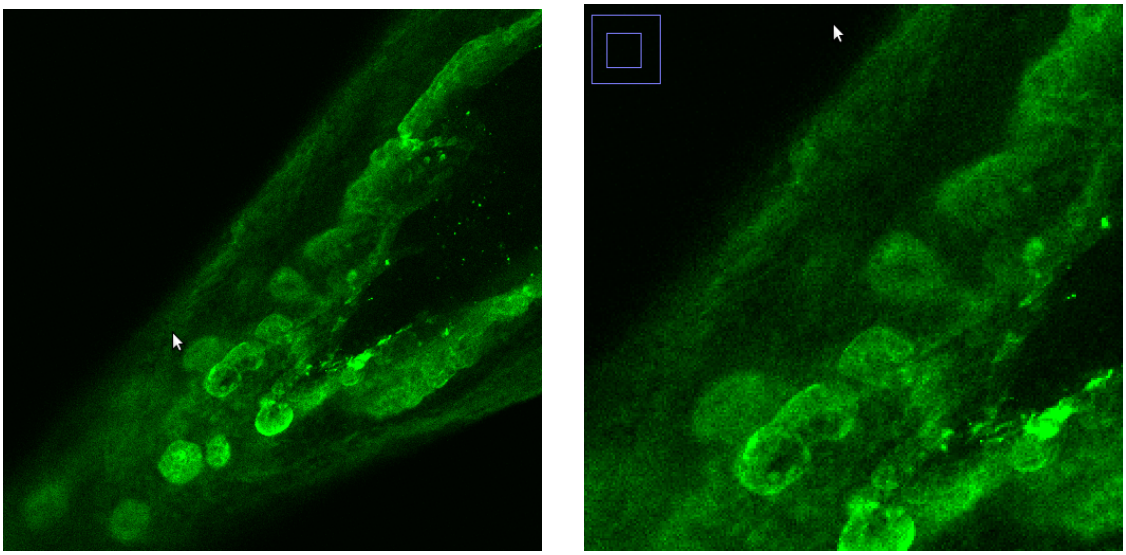

(a) 2D view of original green channel (b) Zoom of 4.1a

Source: Author

Regarding the red channel, the blood vessels are the relevant structures for medical studies. In this channel the presence of noise from the background is also very common, as shown in Figure 4.2a. Some thick blood vessels are well defined but there are other thin vessels that are not easy to differentiate from the background as shown in Figure 4.2b.

When dealing with 3D datasets from images, we must consider whether the 3D images will be directly manipulated. According to (TORIWAKI; YOSHIDA, 2009), the following are some different approaches to keep in mind when making that decision:

1. Applying some processing methodology to a set of independent 2D images and using the result to build or reconstruct the 3D image *(2D image processing with 3D image reconstruction).*

2. Processing each cross section, but during processing take into consideration the status and consistency of neighboring slices (for example, vertical relationships), and using such processing methods as necessary. Sometimes this will be referred to as *2.5D* [1] *processing.*

3. Performing 3D processing on 3D image data *(3D processing).*

[1] 2D image with information that carry some 3D information (2D graphical projections).

Figure 4.2: 2D view of noise in original red channel.

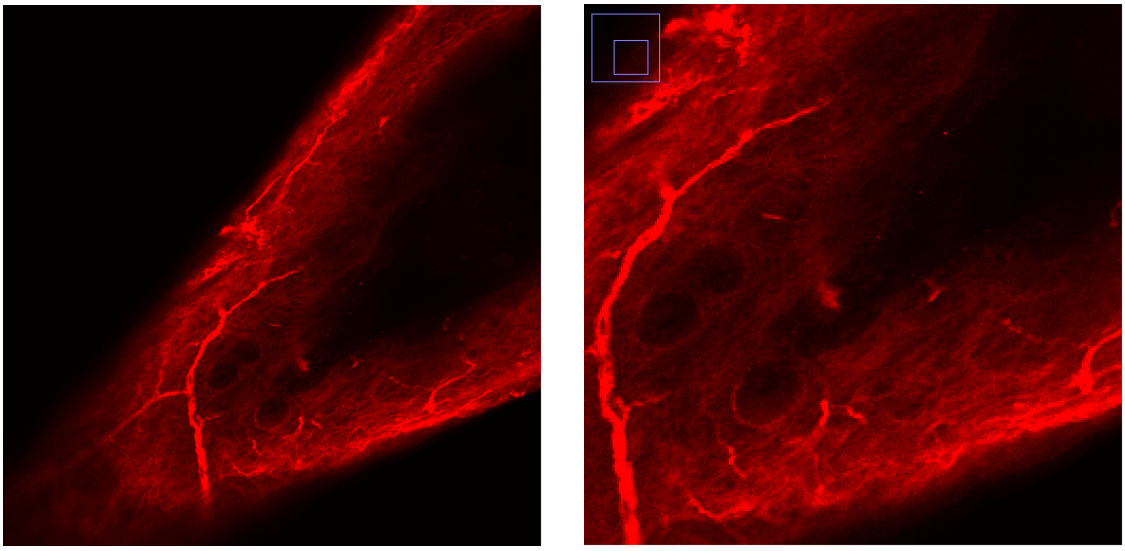

(a) 2D view of original red channel (b) Zoom of 4.2a

Source: Author

In confocal datasets of bile ducts is it difficult to have enough information to process an individual slice without taking into account the previous and subsequent images. In our confocal datasets we noticed that image processing of individual slices would not be an adequate approach because it would not permit to take into account all the information in the dataset. Other limitation on processing the dataset slice by slice is the runtime costs. Based on the three approaches suggested by (TORIWAKI; YOSHIDA, 2009) for processing 3D images and the characteristics of our confocal data, we decided to perform image processing on 3D image data.

Based on the experiments with pre-processing techniques in medical images we decided to use two specific techniques: one for reducing the noise in a first step, and another to enhance relevant structures in a second step. These two techniques are detailed in the next sections.

4.1.1 Image Filtering in the Frequency Domain

We tested some filters in the domain space to reduce noise in our image. However, these filtering processes were very slow with our data due to the high number of images to process in each dataset. Another limitation of using spatial filters on our data was that sometimes they generated artifacts in our images or sometimes removed important structures. To overcome the limitations of filtering in the spatial

domain we explored other domain and, in this context, we studied the frequency domain.

In medical images transforming spatial data into other domains is applied to obtain information that is not readily available in the original acquired data (DOUGHERTY, 2009).

Filtering in the frequency domain allows us to remove noise without creating artifacts in the important structures of the bile ducts, and also allows us to subtract the image background efficiently. In addition to this advantage, filtering in the frequency domain is more efficient (computationally) than filtering in the spatial domain. Considering that our datasets are formed by 192 images or more, we decided to use this technique to reduce noise. We applied the Fourier transform to convert the spatial domain representation of our images into an alternative representation in terms of spatial frequencies as is detailed in Figure 4.3.

The fundamental steps for filtering in frequency domain shown in Figure 4.3, are summarized as follows:

1. Multiply the input image by $(-1)^{x+y}$ to center the transform.
2. Compute $F(u, v)$, the Direct Transfer Function DFT
3. Multiply $F(u, v)$ by a filter function $H(u, v)$
4. Compute the inverse DFT of the result in (3)
5. Obtain the real part of the result in (4)
6. Multiply the result in (5) by $(-1)^{x+y}$

Figure 4.3: Basic steps for filtering in frequency domain.

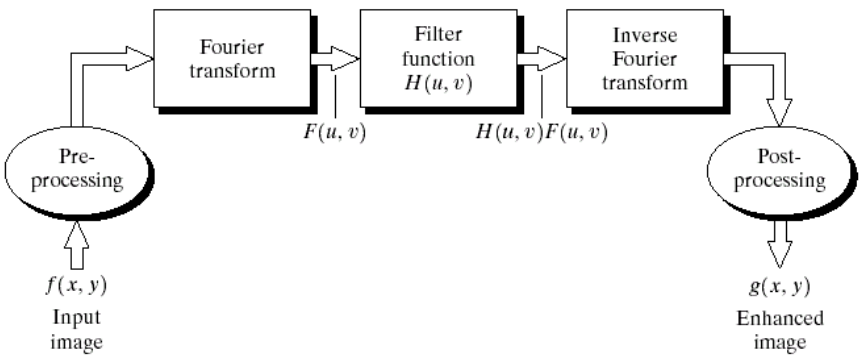

Source: (GONZALEZ; WOODS, 2002)

Figure 4.4: Example of spatial frequency: Shapes which repeat along x axis

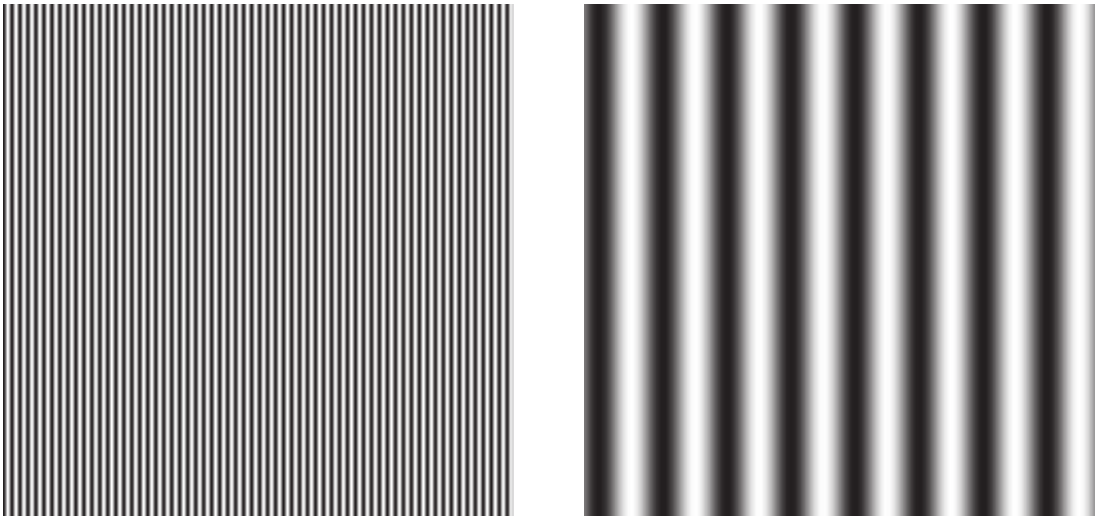

(a) High spatial frequency (b) Low spatial frequency

Source: (DOUGHERTY, 2009)

Spatial frequency is a measure of how frequently intensity values change over distance. High spatial frequencies (Figure 4.4a) are characterized by small repeating distances; intensity values changes from dark to bright to dark over small distances, such as it occurs for fine details like edges or noise in an image. Low spatial frequencies (Figure 4.4b) are characterized by large repeating distances; intensity value changes little with distance, such as it occurs for large objects or the background in an image.

The filter function $H(u, v)$ can be of three types: low-pass filters, high-pass and band-pass filters.

The ideal low-pass filter is used to reduce noise and produce a smoother image. This filter passes all frequencies up to a certain cut-off, k_0 and removes all frequencies beyond that (Figure 4.5). This is described by:

$$\begin{aligned} H(k) &= 1 \quad if \quad k \leq k_0 \\ &= 0 \quad if \quad k > k_0 \end{aligned} \tag{4.1}$$

The ideal high-pass filter is a "brick-wall" filter, which passes all frequencies higher than a certain cut-off frequency, k_0, and removes all frequencies below that

Figure 4.5: Example of low pass filtering in the frequency domain

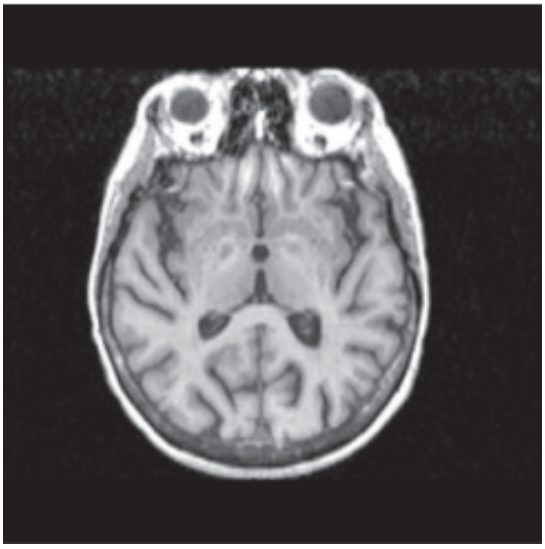

(a) Original image.

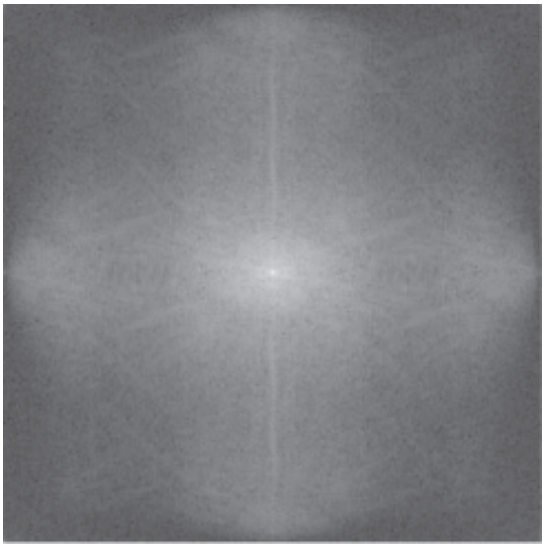

(b) Fourier transform of 4.5a

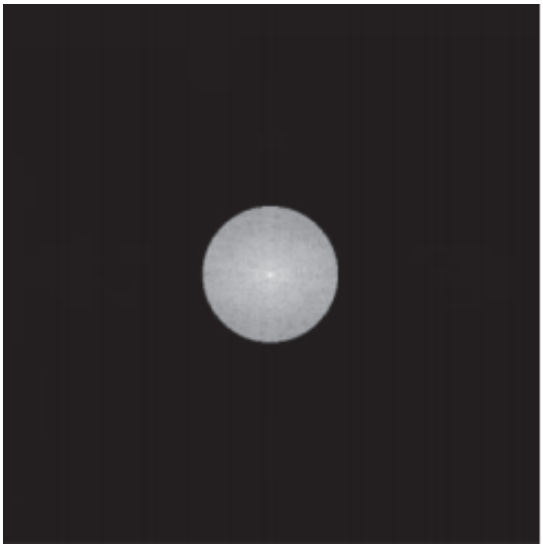

(c) Image 4.5b multiplied by a low pass filter

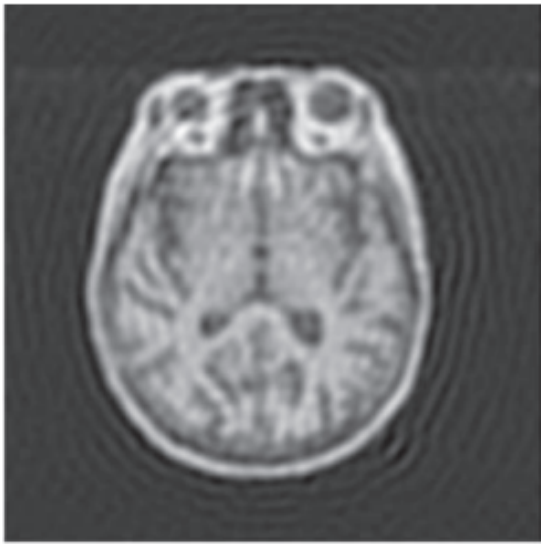

(d) Inverse Fourier transform of 4.5c

Source: (DOUGHERTY, 2009)

(Figure 4.6). It is described by:

$$\begin{aligned} H(k) &= 0 \quad if \quad k \leq k_0 \\ &= 1 \quad if \quad k > k_0 \end{aligned} \tag{4.2}$$

Band-pass filters are a combination of both low-pass and high-pass filters. The result of this combination is shown in Figure 4.7. This filter attenuates smaller and

Figure 4.6: Example of high pass filtering in the frequency domain.

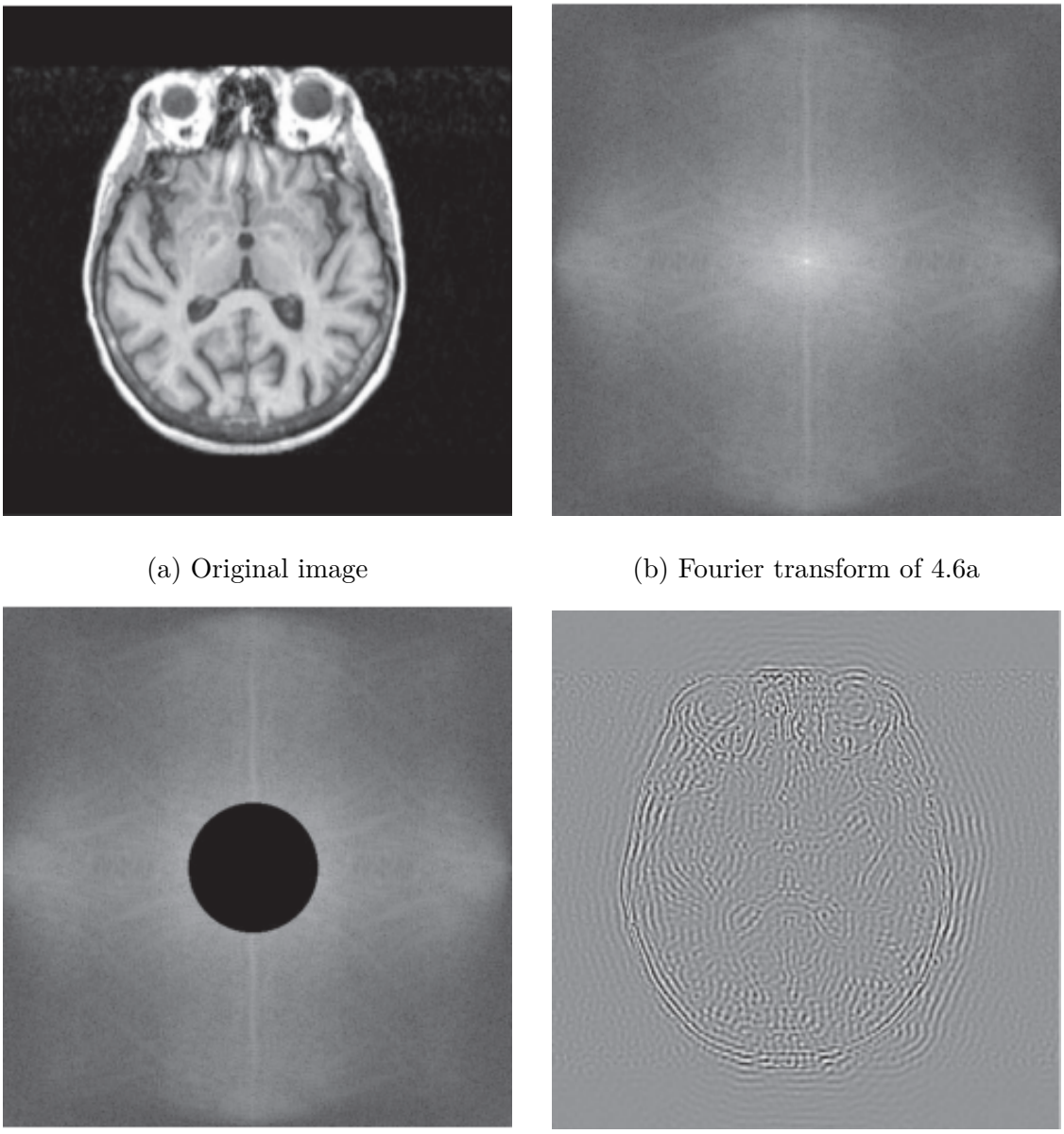

(a) Original image

(b) Fourier transform of 4.6a

(c) Image 4.6b multiplied by a high filter

(d) Inverse Fourier transform of 4.6c

Source: (DOUGHERTY, 2009)

higher frequencies.

We tested the three type of filters in the frequency domain and selected a band pass filter. Band pass filter permits reducing noise of the background and smoothing the data while maintaining the important structures. This type of filters are applied directly in the datasets, and we constructed a volumetric visualization to observe the results. The results of applying this filter to each channel of our data can be seen in Figure 4.8.

Figure 4.7: Example of band pass filtering in the frequency domain.

(a) Band-pass filtered Fourier transform of 4.5a

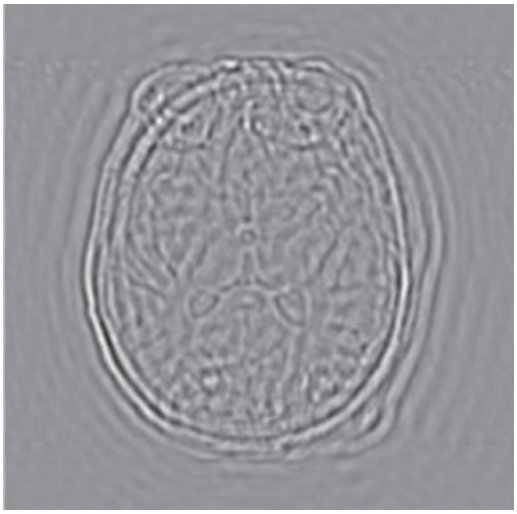

(b) Inverse Fourier transform of 4.7a

Source: (DOUGHERTY, 2009)

4.1.2 Edge Preserving Smoothing via Anisotropic Diffusion

After subtracting the background and reducing the noise by filtering in the frequency domain, we explored and tested filters to enhance the structures present in our datasets.

Traditional linear filters such as Median Filter do not provided significant results to enhance details in our data. That is because they are linear filters performing in all the data, and do not discriminate the important structures.

To overcome the limitations of applying linear filters in our data, we studied non linear filters based on more advanced criteria. After testing some filters by trial and error in our data, we selected the anisotropic diffusion. Anisotropic diffusion is nonlinear filter because this filter is based on the the analysis of partial differential equations (PDEs).

Anisotropic diffusion is a process introduced by (PERONA; MALIK, 1990) for image denoising, based on a principle of dissipating energy with time (YOU et al., 1996). The main advantage of this filter is that this technique is able to reduce noise in an image while trying to preserve sharp edges. The diffusion is anisotropic because it only occurs when a gradient measure is below gradient threshold. Figure 4.9 shows an example of the use of anisotropic diffusion in medical images.

According to (BANKMAN, 2008), the nonlinear anisotropic process can be rep-

resented as shown in Equation 4.3 :

$$\frac{\partial I(\bar{x},t)}{\partial t} = \nabla(c(\bar{x},t)\nabla I(\bar{x},t)) \tag{4.3}$$

Consider $I(\bar{x},t)$ to be the original image where $\bar{x}$ represents the image coordinates *(i.e.,x,y),* t is the iteration step, and $c(\bar{x},t)$, the diffusion function, is a monotonically decreasing function of the image gradient magnitude. Edges can be selectively smoothed or enhanced according the diffusion function. The diffusion function can

Figure 4.8: Filtering our confocal dataset in the frequency domain

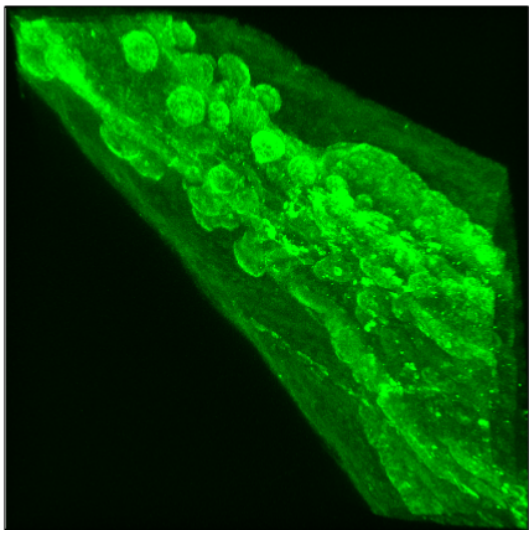

(a) 3D original green channel

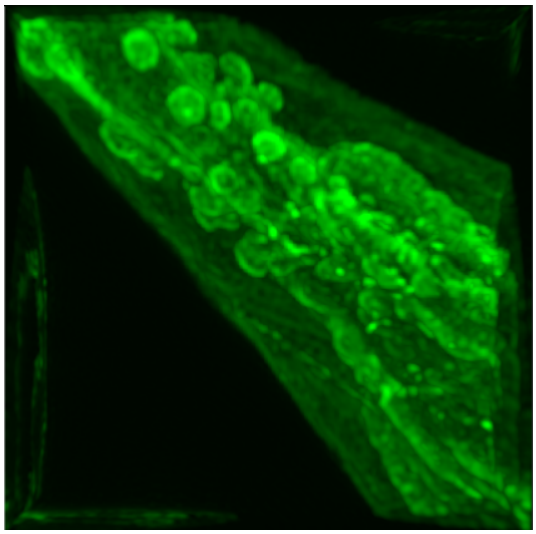

(b) Filtering 4.8a in the frequency domain

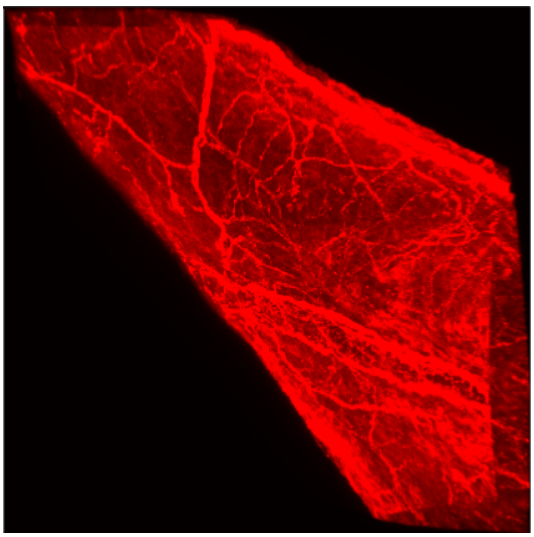

(c) 3D original red channel

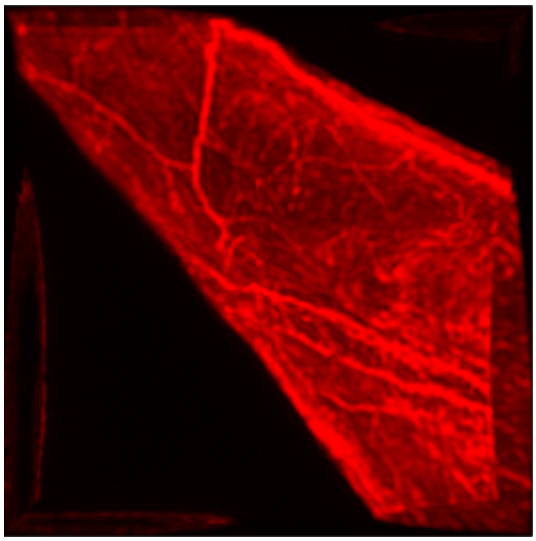

(d) Filtering 4.8c in the frequency domain

Source: Author

be mathematically expressed by the Equation 4.4:

$$c(\bar{x},t) = exp(-(\frac{\mid \nabla I(\bar{x},t) \mid}{\sqrt{2}K})) \tag{4.4}$$

K is the diffusion or flow constant that dictates the behavior of the filter. Good choices of parameters that produce an appropriately blurred image for thresholding are $K = 128$ with 25 iterations and a time step value of just under 0.2.

Figure 4.9 shows an example of the use of anisotropic diffusion in medical data.

Figure 4.9: Example of nonlinear anisotropic diffusion filtering.

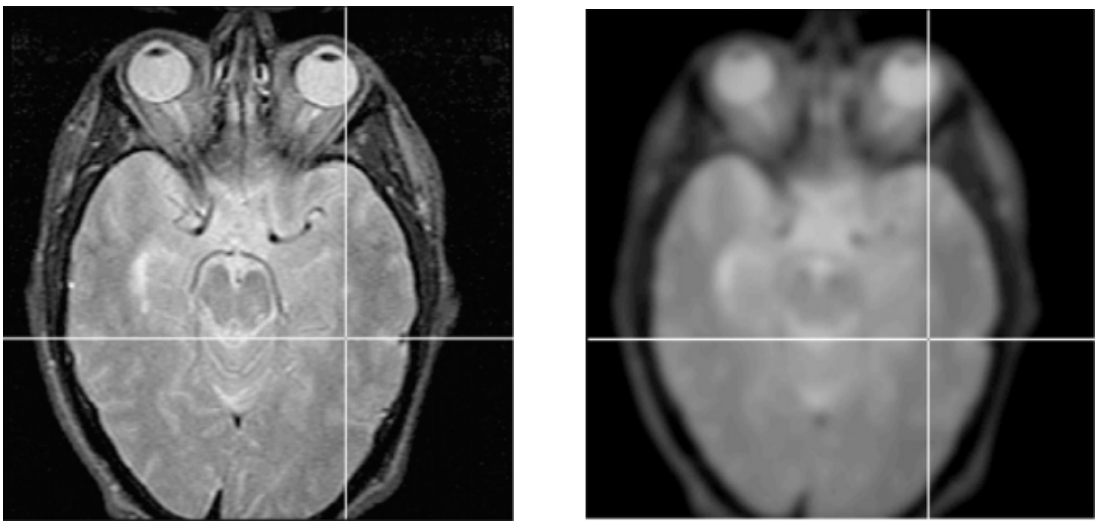

(a) Original image (b) Diffused image

Source: (BANKMAN, 2008)

Figure 4.10 shows an example of the use of anisotropic diffusion in our datasets. In this Figure, we present and intermediate step for visualize the effect of the anisotropic diffusion in the confocal data. Applying anisotropic diffusion in our data offered some advantages to enhance the structures in the bile duct. The edges are enhanced and the background is smoothed. The relevant structures are observed with more details, which permits a better differentiation of the structures from the background.

4.2 Volume Rendering Techniques

We explored volume rendering techniques to construct volumetric visualizations of the pre-processed data.

Figure 4.10: Anisotropic diffusion in our confocal dataset

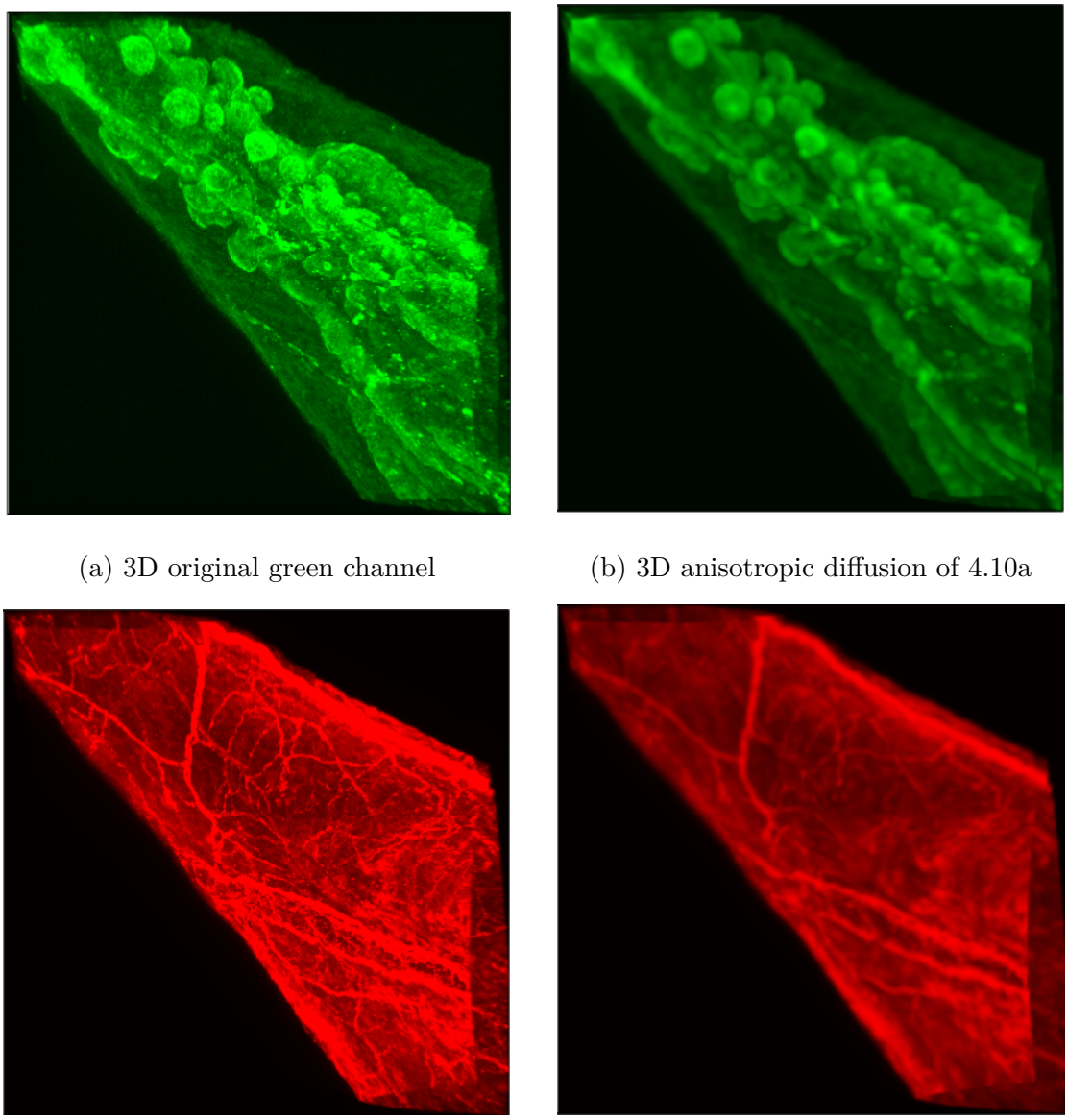

(a) 3D original green channel

(b) 3D anisotropic diffusion of 4.10a

(c) 3D original red channel

(d) 3D anisotropic diffusion of 4.10c

Source: Author

Rendering algorithms are broadly categorized into two groups: indirect and direct volume rendering. Indirect volume rendering uses traditional segmentation algorithms based on thresholding for isolating the structures in a fixed number of parts. Because the nature of our data, algorithms based on thresholding are not the appropriate choice, and for this reason, we discarded the use of indirect volume rendering.

On the other hand, direct volume rendering methods process the volume data based on fuzzy segmentation through transfer functions. This means that one group

of points can belong to more than one structure/tissue with different degrees of membership. Based on the above characteristics we use direct volume rendering techniques to visualize our data. We selected the Ray Casting algorithm (HADWIGER et al., 2006), because this algorithm yielded satisfactory results after the pre-processing step that we proposed.

Although there are other techniques for volume rendering such as those based on textures, this kind of techniques are not appropriate because our data include noise and the structures are difficult to segment.

Our aim with the volumetric visualization was to construct a realistic bile duct, enhancing the original structures and using Ray Casting allowed us to do so.

Volume rendering is based on the emission-absorption optical model defined by the Equation 4.5:

$$I(D) = I_0 e^{-\int_{s_0}^{D} k(t)dt} + \int_{s_0}^{D} q(s) e^{\int_{s}^{D} k(t)dt} ds \tag{4.5}$$

With optical properties k (absorption coefficient) and q (source term describing emission) and integration from entry point into the volume, $s = s_0$, to the exit point toward the camera, $s = D$.

The basic idea of Ray Casting Algorithm is to directly evaluate the volume-rendering integral along rays that are traced from the camera into the object space. For each point in a projection plane (i.e.,for each pixel in the image), a single ray is cast into the volume. Then, the volume data is resampled at discrete positions along the ray. Figure 4.11 illustrates the classical ray casting.

In Figure 4.11, viewing rays are fired through the data to sample the volume. After that, the data is evaluated by using a function in order to compute the final pixel value. The final pixel color is obtained from the accumulation of values obtained using a *transfer function* that maps data values to optical properties.

Direct volume rendering techniques differ considerably in the way they evaluate the Equation 4.5. For solving this equation we need to know the optical properties, such as emission and absorption coefficients, at each point inside the volume. In scientific visualization, however, we are given a volumetric dataset that contains abstract scalar data values that represent some spatial varying physical property. In general, there is no natural way to obtain emission and absorption coefficients from such data. Instead, one has to decide how the different structures in the data should look by assigning optical properties to the data values using arbitrary mappings. This mapping is called *transfer function*. The main advantage of using transfer functions is that we can adjust them to emphasize different structures in our volume. To take advantage of this fact, we used color and opacity values based on a function of the local intensity. As a second dimension, we used the magnitude

Figure 4.11: Ray-casting principle: For each pixel, one viewing ray is traced. The ray is sampled at discrete positions to evaluate the volume-rendering integral

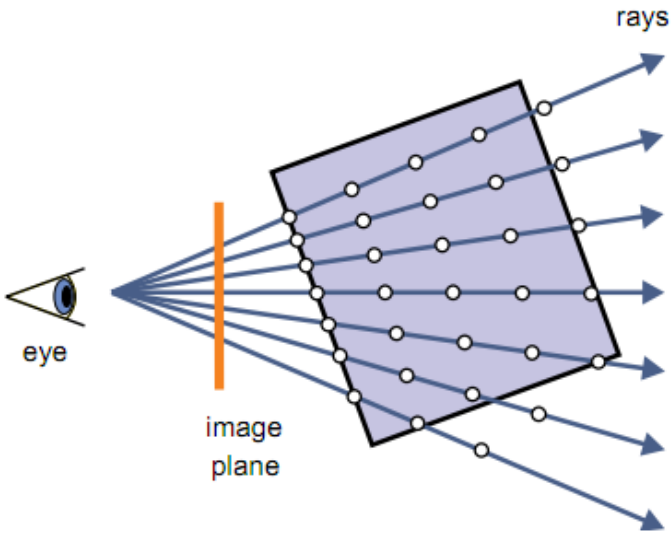

Source: (HADWIGER et al., 2006)

of the gradient vector to emulate the effect of external light sources interacting with tissue boundaries.

The volumetric visualizations presented in this section (Figure 4.8 and the Figure 4.10) were obtained using the ray casting algorithm.

4.3 Proposed Pipeline

We based our proposal on the Visualization ToolKit (VTK) (Kitware Inc., 2014). VTK is an open-source library based on C++ class for 3D computer graphics, image processing and visualization. Because VTK is open source, it has been used in diverse areas including medical visualization, academic research and industrial applications.

Our pipeline provides the visualization of meaningful information from confocal images of bile ducts. The pipeline is composed by two main stages. The first stage involves using the image processing techniques presented in section 4.1, and the second stage is related to the volumetric visualization techniques presented in the section 4.2.

The first stage (Image processing) is needed to overcome limitations in image quality and making the image content more clearly visible for the hepatologists.

The second stage (volumetric visualization) allows the visualization of the three-dimensional structures of the bile duct, and implies the use of the adequate pre-

processing in the first stage.

The pipeline is built from Data Objects (rectangular form in our diagram) and Process Objects (rounded rectangular forms). The Data Object represents our confocal dataset with an organizing structure and the associated attribute data. The Process Objects can be of three types: sources, filters and mappers. The source object is at the beginning of the pipeline, and it represents the reader of the confocal data as shown in Figure 4.12.

Figure 4.12: Developed Pipeline Data Flow

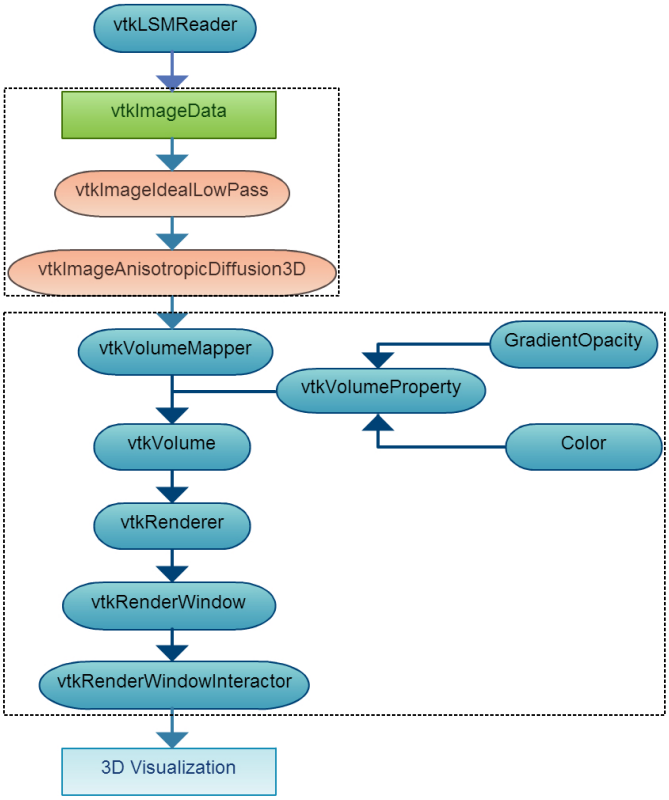

Source: Author

We process the original data format LSM (Laser Scanning Microscopy) to avoid loss of information when converting to another more common format. To read the datasets in LSM format, we use an open source VTK class (*vtkLSMReader*) developed by a research group at University of Turku, Finland (KANKAANPÄÄ et al., 2012), which can be used to support academic research (RODRÍGUEZ et al., 2011). The output of this reader is then connected to the *vtkImageData* object. *VtkImageData* is the basic image data structure in our data flow pipeline. This data object represents the geometric structure of the volume, which is a topological and geometric regular array.

The pipeline continues with the pre-processing step, the first stage for preparing

for visualization. We propose the use of two techniques: filtering in the frequency domain and anisotropic diffusion.

Regarding the filtering in the frequency domain, we use the *vtkImageIdealLowPass* class. This class implements a frequency domain band pass filter that works on an image after it has been converted to frequency domain. As mentioned before, there are other types of filters in the frequency domain. For example, the *vtkImageIdealHighPass* was tested but this filter was not appropriate for our data.

In order to apply an anisotropic diffusion, we use the *vtkImageAnisotropicDiffusion3D* class. *vtkImageAnisotropicDiffusion3D* diffuses the volume iteratively. The diffusion is anisotropic because it only occurs when a gradient measure is below a pre-defined "GradientThreshold".

After the pre-processing step, already in the second stage of the pipeline, there is the mapper class. The mapper is a component of an object named *vtkActor*, which represents a geometrical object and its attributes. In our approach we use volume mappers, which are responsible for the ray casting function and work with all input data from *vtkImageData*. Several basic types of volume mappers are supported. In Chapter 5 we present the results for the mappers selected in this work.

Additional information in the *vtkActor* include the object's appearance attributes (*vtkVolumeProperty*). This class represents common properties associated with volume rendering such as the color and opacity functions. We defined the color transfer function using the *vtkColorTransferFunction* class to map the voxel intensities to RGB color. We used the R and G color components to map the color in the red data and in the green data channel, respectively. For the gradient opacity function we used the *vtkPiecewiseFunction* class to add the control points to construct the function. Other important properties that we defined in this step were the interpolation type and the shade options. We used linear interpolation to obtain a high quality rendering, and the shade options were useful to enhance the appearance of the volume.

Finally, we used VTK renderers to visualize the volume. The *vtkRenderer* allows us to draw the volume, and *vtkRenderWindow* is the container that allows to display the volume in a window on the screen. We added interactivity to the volume rendering output using the *vtkRenderWindowInteractor* class. This class enables mouse events to control the camera's position and orientation. Then, it is possible to display different views of the volumetric bile duct as well as other operations such as rotation and zooming.

4.4 Final Comments

In this chapter we explained our choices for processing and rendering the confocal dataset. We present some partial results to evidence how these techniques operate in the original data and present the pipeline proposed using these techniques.

Next section will present final results as well as the evaluation performed by our expert partner.

5 RESULTS AND EVALUATION

Along the development of this work we have always been in contact with two medical experts, and have shown them the partial results of our visualizations.

As final evaluation of the current pipeline, we selected a confocal volume and showed visualizations to the senior researcher, asking him to perform a thorough qualitative description of the sample. To evaluate different possibilities, we defined different transfer functions for each channel.

The resulting visual description of the data we presented him is summarized in Tables 5.1 and 5.2. For the sake of completeness, we also report here the preliminary visualization we have shown (section 5.1) without the pre-processing stage.

5.1 3D Visualization using color transfer functions

This is referred as "Case 1", where we presented the result of using the ray casting algorithm with a 1D transfer that maps intensity original values to color (Figure 5.1). In this case we used a linear transfer function to map the color in each data channel. We used the RGB color model, and showed only the Red and the Green channel, respectively. Our aim, in this case, was to get a first visualization of the original data, and discuss with the hepatologists the structures that are evidenced with a simple function.

The data channels red and green represent the two structure types that form the bile duct: Peribiliary glands PBGs (in green channel) and Peribiliary vascular plexus PVP (in red channel). This first visualization was used in several discussions with the hepatologists during the development of our work and was the basis for improving the transfer functions and the pipeline itself. Our volumetric visualizations in this case offer a better distinction between the structures than volumetric visualizations constructed with the proprietary software of the confocal microscope presented in the section 3.2

Figure 5.1: Visualization based on color transfer functions.

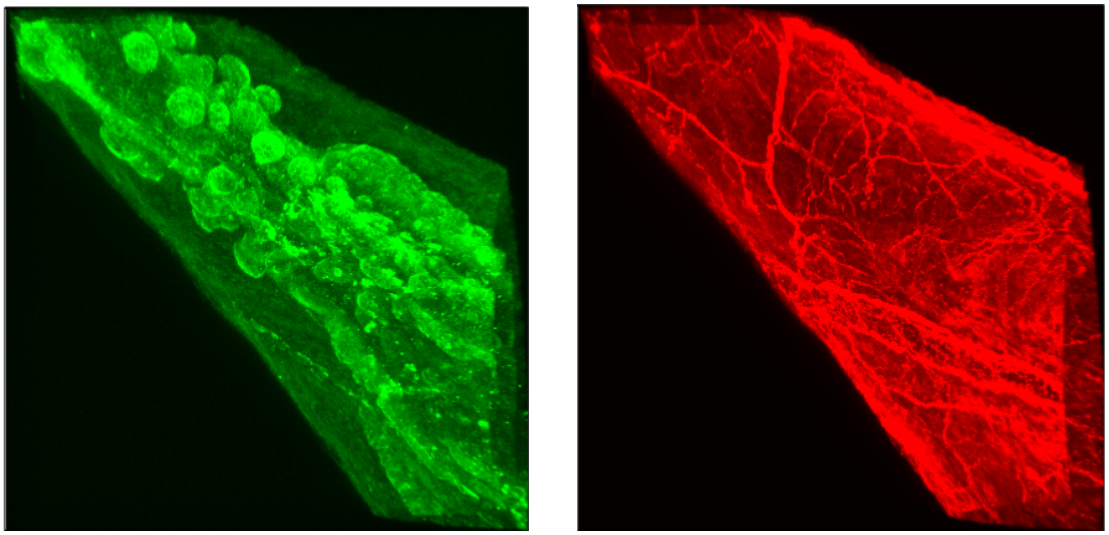

(a) Green channel: Peribiliary glands PBGs. (b) Red Channel: Peribiliar vascular plexus PVP.

Source: Author

5.2 3D Visualization using gradient-based functions after pre-processing

Although the results obtained in Case 1 were considered good in the first evaluations, we found that a pre-processing step was needed to improve image quality.

As mentioned in the Chapter 4, due to the nature of our data we tested and discarded the use of linear filters. To improve the results of the volumetric visualization, we used a filter in the frequency domain and the anisotropic diffusion to reduce noise, while maintaining the important emphasized structures.

So, we devised a gradient-based 2D transfer function and this configured our "Case 2" (Figure 5.2). Our aim was to isolate the regions of interest and improving details found in the original data.

We map the color in the same way explained in the Case 1, but added one more linear transfer function to map the gradient of the dataset into opacity values.

The use of the gradient-based transfer functions allowed to discriminate individual glands (green channel) in order to visualize morphological features, while increasing the distinction between the vessels and the background.

Figure 5.2: Visualization using gradient-based functions after a pre-processing step.

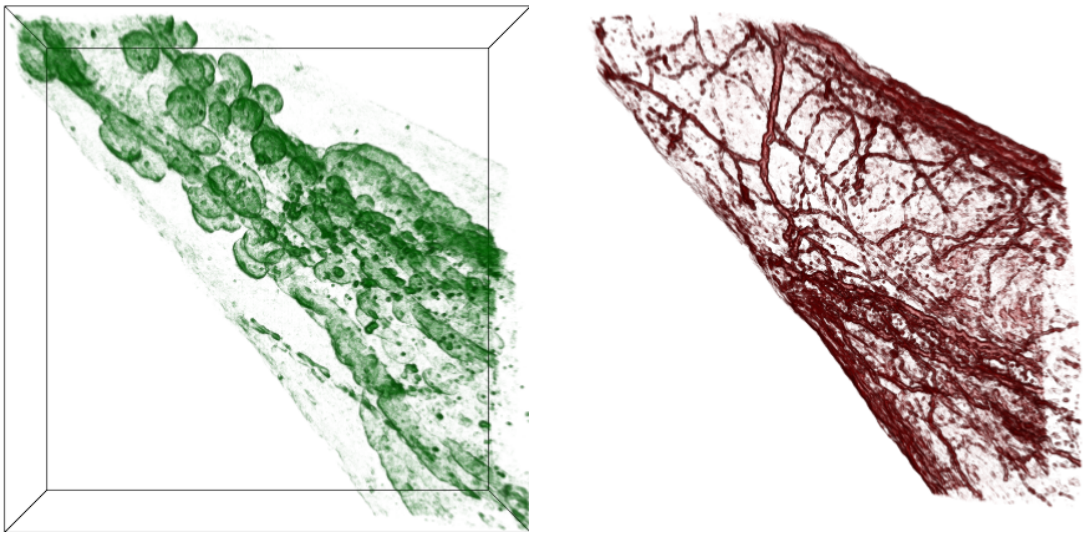

(a) Green channel: Peribiliary glands PBGs (b) Red Channel: Peribiliar vascular plexus PVP.

Source: Author

Figure 5.3: Visualization based on composite functions before pre-processing step.

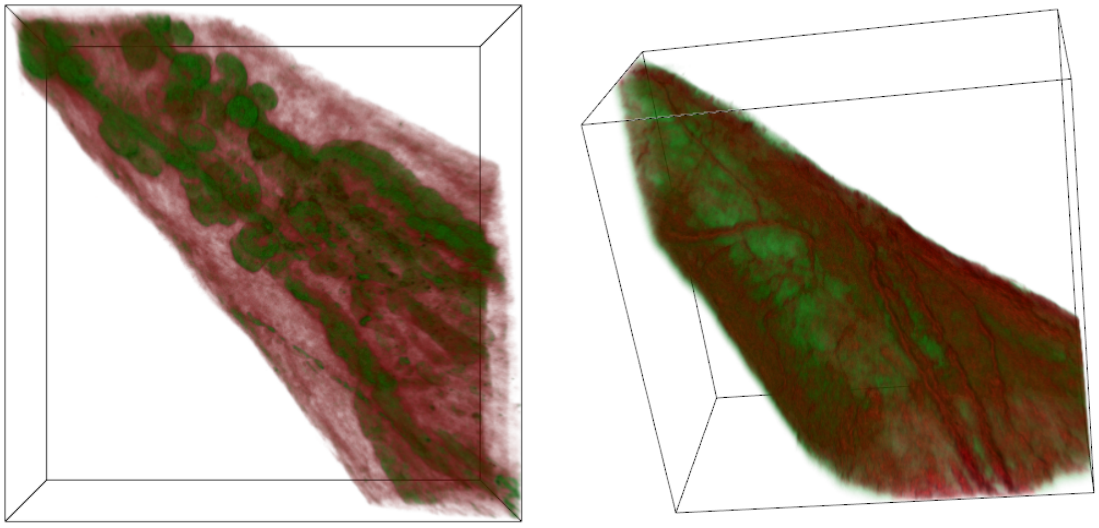

(a) Green channel: Peribiliary glands PBGs (b) Red Channel: Peribiliar vascular plexus PVP.

Source: Author

5.3 3D Visualization based on composite functions after pre-processing

Our "Case 3" (Figure 5.4) was designed with the aim of giving a more realistic aspect to the bile duct.

In this case we have maintained the pre-processing step (filtering in the frequency domain and anisotropic diffusion) but we changed the ray casting function that rendered the data. We used a function that allows to render the volume with an alpha-composite technique. This technique created the appearance of transparency and opacity in our bile duct.

We use linear transfer functions to to map color and opacity.

In this case, we demonstrate the importance of the pre-processing step. Figure 5.3 illustrates the volumetric visualization obtained without the pre-processing step. Figure 5.4b, on the other hand, illustrates that we obtain more details after the pre-processing. We can observe the difference between these visualizations, mainly by the enhanced structures and a more clear distinction between the bile duct structures and the background.

Figure 5.4: Visualization based on alpha-composite functions after pre-processing step.

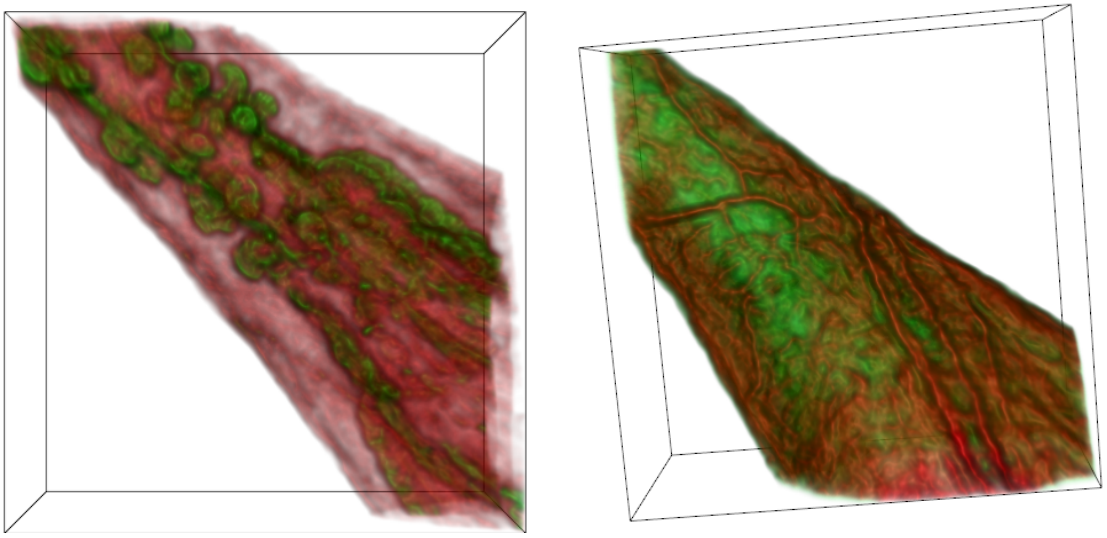

(a) Green channel: Peribiliary glands PBGs (b) Red Channel: Peribiliar vascular plexus PVP.

Source: Author

5.4 Qualitative Evaluation

In this section we present the description of our visualizations made by our senior expert user. We separated each data channel for the visualization and because of this, the descriptions were done in each data channel independently. To the hepatologist, the volumetric visualizations presented in Case 3 solve some problems associated to the original data such as noise and superposition. In addition of these advantages, he also commented that Case 3 maintains clearly discernible the features of the bile duct structures. This last observation is really important because it makes possible the evaluation of morphological alterations in the bile ducts by the hepatologists. The description resulting from his assessment of the three cases are detailed in Tables 5.1 and 5.2.

Table 5.1: Qualitative analysis of the results in the red channel

Case	Visual description by a hepatologist
Case 1	Regarding the red channel in case 1, we observe a strong color superposition between the peribiliary vascular plexus and the background which represents the whole ductal structures
Case 2	Case 2 enables the specification of the peribiliary vascular plexus in relation to the background, thus facilitating the morphometric assessment of the vessels.
Differences between case 1 and 2	The image in case 2, by effacing the background red color, makes easier the characterization of the vascular plexus necessary for specific morphometric analysis.
Case 3	The case 3 maintains clearly discernible the features of both the peribiliary vascular plexus and the ductal structure, giving, additionally, a 3D appearance to the complex of structures under study.
Differences between Case 1, 2 and 3	Case 3 enables the visualization of the ductal structure and its associated peribiliary vascular plexus, solving the blurring between these elements observed in case 1, as well as the excessive effacement of the ductal structure seen in case 2. Additionally, case 3 gives an idea of the 3D configuration of this complex of structures

Source: Author

Those results will be very useful in the next experiments for the hepatologists, which are interested in analyzing several mice bile ducts in different stages of the biliary atresia.

Table 5.2: Qualitative analysis of the results in the green channel

Case	Visual description by a hepatologist
Case 1	We observe the biliary epithelium, including the associated peribiliary glands, more intensely stained in green color, but there is a superposition between epithelium and the remaining tissues, both of them in the same color, thus blurring the anatomical epithelial features of interest.
Case 2	Effaces the background staining, thus making easier to identify the biliary epithelium, specially the peribiliary glands. This is useful for assessing by morphometry the variables of interest involving the peribiliary glands.
Differences between Case 1 and 2	In case 2, by effacement of the background green color, the tissue of interest for the morphometric activity is accentuated.
Case 3	The use of a soft red color for defining the background tissue enabled the characterization of the biliary epithelium and associated peribiliary glands without the strong interference observed with the use of the green channel by the original method, with the advantage of showing the extent of the whole biliary structure that was hidden in case 1.
Differences between case 1,2 and 3	Image presented in case 3 integrates the biliary epithelium and the background tissue that describes the limits of the whole ductal structure, thus making possible to evaluate the morphologic alterations from both these image elements.

Source: Author

6 CONCLUSIONS

In this work, we have proposed a data flow pipeline to construct volumetric visualizations of bile ducts from confocal images. The pipeline is divided into two main sequential stages.

For the first stage we propose an approach to overcome the problem associated to the denoising and enhancing of the relevant structures in the original data. As a second stage, we use the preprocessed data, and apply an approach to construct volumetric visualizations of the bile ducts.

One important contribution in our proposed pipeline was the protocol for the pre-processing of the original datasets. Usually for data acquired from images, the adequate techniques and the order to applying them are very dependent of the type of data. We have observed a lack of computational methods for confocal images in the literature as well as in the existing plethora of image processing and visualization software.

Confocal data has not been treated by existing applications, and related work in visualization of confocal dataset do not describe pre-processing steps. The techniques we used were selected after several tests of different filtering techniques and this was a task that took the most part of the time dedicated to the work. By applying our pipeline in the confocal datasets of bile ducts, we have isolated regions of interest and make possible the visualization of details that were hardly visualized in the original data.

Our results so far offered some advantages for the hepatologists in the study of the bile duct structures.

As reported by the experts during the development of this work and in the final round of qualitative evaluation, the identification of relevant structures were more easily performed in our volumetric visualizations, and that made possible a more detailed qualitative analysis of the bile ducts. Those qualitative analysis are very important in the study of the bile ducts structures in different stages of the biliary atresia. Once they have several datasets, showing different stages of the development of the disease, they will be able to analyze the changes in morphology, distribution,

number and size of the samples.

In addition to the visual improvement in the confocal data, other advantages of our pipeline is that it was developed using an open-source library and is capable of read the LSM file format produced from confocal microscopes. Reading the LSM file format made possible the access to the original datasets, allowing to take advantage from the way in which the data was collected.

As for future work, there are several possibilities. We intend to further improve pre-processign techniques with datasets that show different stages of biliary atresia, when they are available.

Regarding visualization, we aim at studying and testing additional attributes to build volumetric visualizations using multidimensional transfer functions.

Finally, we also intend to develop interactive techniques for helping the medical experts in their analysis, for example, by counting peribiliary glands, measuring their size, and probably devising some shape analysis of the vascular plexus.

REFERENCES

BANKMAN, I. **Handbook of medical image processing and analysis**. [S.l.]: Academic press, 2008. 2 citations in pages 40 and 42.

BEYER, J. et al. Connectomeexplorer: Query-guided visual analysis of large volumetric neuroscience data. **IEEE Transactions on Visualization and Computer Graphics**, IEEE Educational Activities Department, Piscataway, NJ, USA, v. 19, n. 12, p. 2868–2877, dec. 2013. ISSN 1077-2626. One citation in page 24.

CLAXTON, N. S.; FELLERS, T. J.; DAVIDSON, M. W. Laser scanning confocal microscopy. **Department of Optical Microscopy and Digital Imaging, The Florida State University, Tallahassee, Florida**, 2006. One citation in page 13.

CLAXTON, N. S.; FELLERS, T. J.; DAVIDSON, M. W. Laser scanning confocal microscopy. **Department of Optical Microscopy and Digital Imaging, National High Magnetic Field Laboratory, The Florida State University**, 2006. 3 citations in pages 13, 17, and 21.

DEMARTINES, N. et al. Evaluation of magnetic resonance cholangiography in the management of bile duct stones. **Archives of Surgery**, American Medical Association, v. 135, n. 2, p. 148–152, 2000. One citation in page 22.

DIPAOLA, F. et al. Identification of intramural epithelial networks linked to peribiliary glands that express progenitor cell markers and proliferate after injury in mice. **Hepatology: Official Journal of the American Association for the Study of Liver Diseases**, 2013. 4 citations in pages 13, 14, 26, and 28.

DOUGHERTY, G. **Digital image processing for medical applications**. [S.l.]: Cambridge University Press, 2009. 5 citations in pages 36, 37, 38, 39, and 40.

DREBIN, R. A.; CARPENTER, L.; HANRAHAN, P. Volume rendering. **SIGGRAPH Comput. Graph.**, ACM, New York, NY, USA, v. 22, n. 4, p. 65–74, jun. 1988. ISSN 0097-8930. One citation in page 13.

GONZALEZ, R. C.; WOODS, R. E. **Digital Image Processing (3rd Edition)**. Upper Saddle River, NJ, USA: Prentice-Hall, Inc., 2002. ISBN 013168728X. One citation in page 36.

HADWIGER, M. et al. **Real-time Volume Graphics**. Natick, MA, USA: A. K. Peters, Ltd., 2006. ISBN 1568812663. 2 citations in pages 44 and 45.

HOPWOOD, D.; WOOD, R.; MILNE, G. The fine structure and histochemistry of human bile duct in obstruction and choledocholithiasis. **The Journal of pathology**, Wiley Online Library, v. 155, n. 1, p. 49–59, 1988. One citation in page 28.

HORROW, M. M. Ultrasound of the extrahepatic bile duct: issues of size. **Ultrasound quarterly**, LWW, v. 26, n. 2, p. 67–74, 2010. One citation in page 22.

INOUÉ, S. Microtubule dynamics in cell division: exploring living cells with polarized light microscopy. **Annual review of cell and developmental biology**, Annual Reviews, v. 24, p. 1–28, 2008. One citation in page 24.

JOE, K.; GORDON, K.; CHARLES, H. Multidimensional transfer functions for interactive volume rendering. **IEEE Transactions on Visualization and Computer Graphics**, IEEE Educational Activities Department, Piscataway, NJ, USA, v. 8, n. 3, p. 270–285, jul. 2002. ISSN 1077-2626. One citation in page 24.

KANKAANPÄÄ, P. et al. Bioimagexd: an open, general-purpose and high-throughput image-processing platform. **Nature methods**, Nature Publishing Group, v. 9, n. 7, p. 683–689, 2012. One citation in page 46.

KIM, H. S. **Visual Exploration in Volume Rendering for Multi-channel Data**. Thesis (PhD), University of California at San Dieg, La Jolla, CA, USA, 2011. One citation in page 24.

KIM, H. S. et al. **Multichannel transfer function with dimensionality reduction**. 2010. 75300A-75300A-12 p. 2 citations in pages 24 and 25.

KINDLMANN, G.; DURKIN, J. W. Semi-automatic generation of transfer functions for direct volume rendering. In: IEEE SYMPOSIUM ON VOLUME VISUALIZATION. **Proceedings...** New York, NY, USA: ACM, 1998. (VVS '98), p. 79–86. ISBN 1-58113-105-4. One citation in page 24.

Kitware Inc. **The Visualization Toolkit (VTK)**. 2014. <http://www.vtk.org/>. Accessed on: March 2014. One citation in page 45.

KNISS, J.; KINDLMANN, G.; HANSEN, C. Interactive volume rendering using multi-dimensional transfer functions and direct manipulation widgets. In: CONFERENCE ON VISUALIZATION '01. **Proceedings...** Washington, DC, USA: IEEE Computer Society, 2001. (VIS '01), p. 255–262. ISBN 0-7803-7200-X. One citation in page 24.

LONG, F. et al. A 3d digital atlas of c. elegans and its application to single-cell analyses. **Nature methods**, Nature Publishing Group, v. 6, n. 9, p. 667–672, 2009. One citation in page 24.

LONG, F.; ZHOU, J.; PENG, H. Visualization and analysis of 3d microscopic images. **PLoS computational biology**, Public Library of Science, v. 8, n. 6, p. e1002519, 2012. One citation in page 24.

LUM, E.; MA, K.-L. Lighting transfer functions using gradient aligned sampling. In: **Visualization, 2004. IEEE**. [S.l.: s.n.], 2004. p. 289–296. One citation in page 24.

MEIJERING, E. et al. Design and validation of a tool for neurite tracing and analysis in fluorescence microscopy images. **Cytometry Part A**, Wiley Online Library, v. 58, n. 2, p. 167–176, 2004. One citation in page 24.

Michael W. Davidson. **Basic Concepts in Fluorescence**. 2014. <http://micro.magnet.fsu.edu/primer/techniques/fluorescence/fluorescenceintro.html>. Accessed on: November 2014. One citation in page 16.

PENG, H.; LONG, F.; MYERS, G. Automatic 3d neuron tracing using all-path pruning. **Bioinformatics**, Oxford Univ Press, v. 27, n. 13, p. i239–i247, 2011. One citation in page 24.

PENG, H. et al. Automatic reconstruction of 3d neuron structures using a graph-augmented deformable model. **Bioinformatics**, Oxford Univ Press, v. 26, n. 12, p. i38–i46, 2010. One citation in page 24.

PERONA, P.; MALIK, J. Scale-space and edge detection using anisotropic diffusion. **Pattern Analysis and Machine Intelligence, IEEE Transactions on**, IEEE, v. 12, n. 7, p. 629–639, 1990. One citation in page 40.

PINTO, F. d. M.; FREITAS, C. M. D. S. Volume visualization and exploration through flexible transfer function design. **Comput. Graph.**, Pergamon Press, Inc., Elmsford, NY, USA, v. 32, n. 4, p. 420–429, aug. 2008. ISSN 0097-8493. One citation in page 24.

PRICE, R. L.; JEROME, W. G. **Basic Confocal Microscopy**. New York: Springer, 2011. ISBN 978-1-84800-173-2. 6 citations in pages 13, 16, 18, 19, 22, and 26.

RAFALSKA-METCALF, I. U.; JANICKI, S. M. Show and tell: visualizing gene expression in living cells. **Journal of cell science**, The Company of Biologists Ltd, v. 120, n. 14, p. 2301–2307, 2007. One citation in page 24.

RAMESH, N.; OTSUNA, H.; TASDIZEN, T. Three-dimensional alignment and merging of confocal microscopy stacks. In: 20TH IEEE INTERNATIONAL CONFERENCE ON IMAGE PROCESSING (ICIP). **Proceedings...** [S.l.], 2013. p. 1447–1450. One citation in page 27.

RODRÍGUEZ, N. D. et al. Programming biomedical smart space applications with bioimagexd and pythonrules. In: PASCHKE, A. et al. (Ed.). **4th International Workshop on Semantic Web Applications and Tools for the Life Sciences (SWAT4LS 2011)**. [S.l.]: ACM, 2011. p. 10–11. One citation in page 46.

RUBEL, O. et al. Integrating data clustering and visualization for the analysis of 3d gene expression data. **Computational Biology and Bioinformatics, IEEE/ACM Transactions on**, IEEE, v. 7, n. 1, p. 64–79, 2010. One citation in page 24.

SANTOS, J.; CARVALHO, E.; BEZERRA, J. Advances in biliary atresia: from patient care to research. **Brazilian Journal of Medical and Biological Research**, v. 43, p. 522 – 527, 06 2010. One citation in page 13.

SUZUKI, M. et al. Ct diagnosis of common bile duct stone. **Gastrointestinal Radiology**, Springer-Verlag, v. 8, n. 1, p. 327–331, 1983. ISSN 0364-2356. One citation in page 22.

TERADA, T.; KIDA, T.; NAKANUMA, Y. Extrahepatic peribiliary glands express *alpha*-amylase isozymes, trypsin and pancreatic lipase: An immunohistochemical analysis. **Hepatology**, W.B. Saunders, v. 18, n. 4, p. 803–808, 1993. ISSN 1527-3350. Available from Internet: <http://dx.doi.org/10.1002/hep.1840180409>. One citation in page 28.

TORIWAKI, J.; YOSHIDA, H. **Fundamental of Three Dimensional Digital Image Processing**. New York: Springer, 2009. ISBN 978-0-387-78175-4. 5 citations in pages 19, 20, 23, 34, and 35.

WAN, Y. et al. Fluorender: An application of 2d image space methods for 3d and 4d confocal microscopy data visualization in neurobiology research. In: IEEE PACIFIC VISUALIZATION SYMPOSIUM (PACIFICVIS). **Proceedings...** [S.l.], 2012. p. 201–208. ISSN 2165-8765. 2 citations in pages 16 and 24.

YOU, Y.-L. et al. Behavioral analysis of anisotropic diffusion in image processing. **Image Processing, IEEE Transactions on**, v. 5, n. 11, p. 1539–1553, Nov 1996. ISSN 1057-7149. One citation in page 40.

ZEISS, C. **ZEN Light Edition Software, v1.5.5**. Jena: Zeiss, 2009. <http://zen-2009-light-edition.software.informer.com/download/>. Accessed on: April 2014. 2 citations in pages 31 and 32.